



Article

Less Severe Sepsis in Cecal Ligation and Puncture Models with and without Lipopolysaccharide in Mice with Conditional *Ezh2*-Deleted Macrophages (LysM-Cre System)

Pornpimol Phuengmaung ^{1,2}, Phuriwat Khiewkamrop ^{3,4}, Jiradej Makjaroen ⁵ , Jiraphorn Issara-Amphorn ⁶,
Atsadang Boonmee ⁷, Salisa Benjaskulluecha ⁷, Patcharee Ritprajak ⁸ , Aleksandra Nita-Lazar ⁶ ,
Tanapat Palaga ^{3,7}, Nattiya Hirankarn ^{2,3,*} and Asada Leelahavanichkul ^{1,2,9,*}

- ¹ Center of Excellence in Translational Research in Inflammation and Immunology (CETRII), Faculty of Medicine, Chulalongkorn University, Bangkok 10330, Thailand; pphuengmaung@gmail.com
- ² Department of Microbiology, Faculty of Medicine, Chulalongkorn University, Bangkok 10330, Thailand
- ³ Center of Excellence in Immunology and Immune-Mediated Diseases, Chulalongkorn University, Bangkok 10330, Thailand; phuriwat.khi@gmail.com (P.K.); tanapat.palaga@gmail.com (T.P.)
- ⁴ Medical Microbiology, Interdisciplinary and International Program, Graduate School, Chulalongkorn University, Bangkok 10330, Thailand
- ⁵ Center of Excellence in Systems Biology, Research Affairs, Faculty of Medicine, Chulalongkorn University, Bangkok 10330, Thailand; jiradejmak@gmail.com
- ⁶ Functional Cellular Networks Section, Laboratory of Immune System Biology, National Institute of Allergy and Infectious Diseases, National Institutes of Health, Bethesda, MD 20892, USA; jiraphorn.issara-amphorn@nih.gov (J.I.-A.); nitalazarau@niaid.nih.gov (A.N.-L.)
- ⁷ Department of Microbiology, Faculty of Science, Chulalongkorn University, Bangkok 10330, Thailand; atsadang88@gmail.com (A.B.); salisafaii@gmail.com (S.B.)
- ⁸ Research Unit in Integrative Immuno-Microbial Biochemistry and Bioresponsive Nanomaterials, Department of Microbiology, Faculty of Dentistry, Chulalongkorn University, Bangkok 10330, Thailand; p.ritprajak@gmail.com
- ⁹ Division of Nephrology, Department of Medicine, Faculty of Medicine, Chulalongkorn University, Bangkok 10330, Thailand
- * Correspondence: nattiya.h@chula.ac.th (N.H.); aleelahavanit@gmail.com (A.L.); Tel.: +66-22-564-132 (N.H. & A.L.)



Citation: Phuengmaung, P.; Khiewkamrop, P.; Makjaroen, J.; Issara-Amphorn, J.; Boonmee, A.; Benjaskulluecha, S.; Ritprajak, P.; Nita-Lazar, A.; Palaga, T.; Hirankarn, N.; et al. Less Severe Sepsis in Cecal Ligation and Puncture Models with and without Lipopolysaccharide in Mice with Conditional *Ezh2*-Deleted Macrophages (LysM-Cre System). *Int. J. Mol. Sci.* **2023**, *24*, 8517. <https://doi.org/10.3390/ijms24108517>

Academic Editor: Paolo Iadarola

Received: 8 April 2023

Revised: 2 May 2023

Accepted: 7 May 2023

Published: 10 May 2023



Copyright: © 2023 by the authors. Licensee MDPI, Basel, Switzerland. This article is an open access article distributed under the terms and conditions of the Creative Commons Attribution (CC BY) license (<https://creativecommons.org/licenses/by/4.0/>).

Abstract: Despite a previous report on less inflammatory responses in mice with an absence of the enhancer of zeste homologue 2 (*Ezh2*), a histone lysine methyltransferase of epigenetic regulation, using a lipopolysaccharide (LPS) injection model, proteomic analysis and cecal ligation and puncture (CLP), a sepsis model that more resembles human conditions was devised. As such, analysis of cellular and secreted protein (proteome and secretome) after a single LPS activation and LPS tolerance in macrophages from *Ezh2* null (*Ezh2*^{fl^{ox}/fl^{ox}}; *LysM-Cre*^{cre/-}) mice (*Ezh2* null) and the littermate control mice (*Ezh2*^{fl/fl}; *LysM-Cre*^{-/-}) (*Ezh2* control) compared with the unstimulated cells from each group indicated fewer activities in *Ezh2* null macrophages, especially by the volcano plot analysis. Indeed, supernatant IL-1 β and expression of genes in pro-inflammatory M1 macrophage polarization (*IL-1 β* and *iNOS*), *TNF- α* , and *NF- κ B* (a transcription factor) were lower in *Ezh2* null macrophages compared with the control. In LPS tolerance, downregulated *NF- κ B* compared with the control was also demonstrated in *Ezh2* null cells. In CLP sepsis mice, those with CLP alone and CLP at 2 days after twice receiving LPS injection, representing sepsis and sepsis after endotoxemia, respectively, symptoms were less severe in *Ezh2* null mice, as indicated by survival analysis and other biomarkers. However, the *Ezh2* inhibitor improved survival only in CLP, but not LPS with CLP. In conclusion, an absence of *Ezh2* in macrophages resulted in less severe sepsis, and the use of an *Ezh2* inhibitor might be beneficial in sepsis.

Keywords: sepsis; lipopolysaccharide; macrophages; epigenetics; *Ezh2*

1. Introduction

Sepsis is a potentially life-threatening condition in response to severe infection regardless of the organismal causes of the infection [1–3], which is roughly divided into the hyperinflammation stage and immune exhaustion (immune paralysis) phase [4,5]. Sepsis-induced hyperinflammation is a well-known cause of sepsis mortality, partly through hypercytokinemia-mediated septic shock, especially at an early phase of sepsis [6]. Meanwhile, sepsis-induced immune exhaustion is developed at the same time or shortly after the hyperinflammation, at least in part, due to immune cell death from overwhelming responses against several stimulators from the pathogens and hosts, referred to as pathogen-associated molecular patterns (PAMPs) and damage-associated molecular patterns (DAMPs), respectively [6]. Subsequently, an inadequate response to control the organism during sepsis-induced immune exhaustion results in another episode of secondary infection and another episode of septic shock from the different pathogens [7]. Due to the opposite direction of immune responses in different phases of sepsis, different strategic treatments are necessary. As such, an anti-inflammatory treatment might be beneficial for sepsis-hyperinflammation to attenuate the unnecessary overwhelming immune responses that might be harmful to the host. Meanwhile, an escalation of immune responsiveness during immune exhaustion may be helpful to enhance the microbial control ability of the host to prevent secondary infections [8–15]. Despite the successful decrease in short-term sepsis mortality due to improved supportive care, immune exhaustion-induced secondary infection seems to become more common [16]. Indeed, immune cell apoptosis, myeloid-derived suppressor cells, regulatory T cells, and lipopolysaccharide (LPS) tolerance are mentioned as underlying mechanisms of sepsis-induced immune exhaustion [17–20]. Among these topics, data on LPS tolerance in sepsis are relatively fewer compared with those on other mechanisms. The presence of LPS, a major molecule of Gram-negative bacteria, in blood circulation during sepsis (endotoxemia) is common due to Gram-negative bacterial infection and/or the translocation of LPS from the intestine into the blood circulation, referred to as “leaky gut”, and is a common cause of endotoxemia [21–23]. Because of the highest abundance of Gram-negative bacteria in the gut compared with other organisms, endotoxemia from a leaky gut is mentioned in several conditions with gut barrier defects, including sepsis [1–3]. Subsequently, an adaptation to the prolonged LPS stimulations in sepsis may initiate LPS tolerance [24,25]. Among several models of sepsis, cecal ligation and puncture (CLP) is a standard model used for sepsis hyper-inflammation [14,23,26–29] that more resembles the human condition than a single LPS injection [30]. Meanwhile, sepsis immune exhaustion consists of several models, based on increased susceptibility of the secondary infection [31,32], and the more severe sepsis in CLP surgery after LPS tolerance, using twice-administered LPS injection, compared with CLP without LPS pre-conditioning is previously mentioned [25]. Indeed, the more severe sepsis, especially bacteremia, in CLP after LPS tolerance compared with CLP alone is matched with the common characteristic of the worsened infection in sepsis-induced immune exhaustion compared with the normal immune regulation [33]. Then, CLP and CLP after LPS tolerance were used as models of hyperinflammation and LPS tolerance-associated immune exhaustion with sepsis, respectively.

Interestingly, the tolerance against LPS, especially in monocytes or macrophages, is possibly due to the epigenetic modifications, chromatin remodeling, and interferences in cell energy status [34–36], among which epigenetic alteration is the most extensively studied [37,38]. Epigenetics is the phenotypic alterations without the changes in the DNA sequence for the switch “on” and “off” of DNA transcription through (i) the modifications of DNA and/or histone through several enzymes [3,39], and (ii) noncoding RNA (microRNA) [2]. Among

all, the methylation at histone 3 lysine 27 (H3K27) is one of the most common epigenetic processes through histone changes for several cell activities, including after LPS activation [40]. In LPS-activated macrophages, the insertion of methyl groups at lysine 27 on histone 3 (H3K27) by histone demethylase is controlled by the polycomb repressor complex group 2 (PCR2), a repressor molecule consisting of several subunits, including Ezh2 (histone-lysine N-methyltransferase-2 or enhancer of zeste homolog) [41,42], to switch off the DNA transcription (reduce cytokine production) through this histone modification [43,44]. Due to the important Ezh2 catalytic activity on PCR2, Ezh2 overexpression enhances PCR2 inhibitory function with an anti-inflammatory effect [45,46] and Ezh2 deletion should enhance pro-inflammatory responses [47]. Indeed, the enhanced pro-inflammatory effect of Ezh2 blockage is mentioned via (i) increased tumoricidal impact of tazemetostat (an Ezh2 inhibitor) [48] and (ii) worsened colitis after *Ezh2* downregulation [49]. In contrast, the anti-inflammatory property of Ezh2 blockage is also mentioned in the atherosclerosis model [50]. Hence, Ezh2 not only downregulates pro-inflammatory cytokines but also can decrease the anti-inflammatory process, partly through the downregulation of the suppressor of cytokine signaling 3 (*Socs3*) [51]. Ezh2 causes histone methylation that block transcription of both pro-inflammatory genes (cytokines) and anti-inflammatory genes (*Socs3*) and the impact of Ezh2 might be different among various genes and cell types. Indeed, in mice with conditional Ezh2 deletion by the LysM-Cre system, Ezh2 deletion only in the myeloid cells (monocytes, macrophages, and neutrophils) demonstrates less severe responses against a single LPS injection, but not LPS tolerance (two LPS injections), and bone marrow-derived macrophages from these mice indicated less potent LPS responses (lower supernatant cytokines) and less severe LPS tolerance (higher supernatant cytokines) compared with the control cells [39]. Although Ezh2 impacts on sepsis are still inconclusive, Ezh2 is one of the upregulated genes in LPS-tolerant macrophages [52] which is improved by the Ezh2 inhibitor (enhanced TNF- α expression) [53] as an interesting control of macrophage through epigenetic manipulation [13,54].

Here, the influence of Ezh2 on LPS was further explored through proteomic analysis and tested in a model with sepsis hyper-inflammatory responses (CLP) and a sepsis model after LPS tolerance (twice-administered LPS injection before CLP surgery) using the conditional Ezh2 deletion mice and an Ezh2 inhibitor.

2. Results

2.1. Proteomic Analysis of Lipopolysaccharide (LPS)-Induced Macrophages from Control and Ezh2 Null Mice

The difference in bone marrow-derived macrophage (BMDM) after activation with three protocols, namely control, a single LPS stimulation, and LPS tolerance (Figure 1A), of macrophages from Ezh2 control (*Ezh2^{fl/fl}; LysM-Cre^{-/-}*) or Ezh2 null (*Ezh2^{fl/fl}; LysM-Cre^{cre/-}*) mice were analyzed by proteome and secretome, using the cells and cell supernatant, respectively. With a single LPS stimulation, there were prominent alterations in the peptides of Ezh2 control macrophages compared with the neutral state of Ezh2 control cells as indicated by the up- and downregulation at 188 and 119 proteins, respectively (Figure 1B, left upper). Meanwhile, the values of LPS-activated Ezh2 null cells were 32 and 9 proteins, respectively (Figure 1B, lower left), suggesting possible less activity of Ezh2 null macrophages compared with that in the cells from littermate control mice. Likewise, the up- and downregulated molecules in LPS tolerance of Ezh2 control macrophages compared with the neutral state were 392 and 296 proteins, respectively (Figure 1B, upper right), while for the Ezh2 null cells they were 107 and 68 proteins, respectively (Figure 1B, lower

right). With the fold enrichment pathway analysis (ShinyGo 0.77), most of the proteins were correlated to immune response pathways and cell energy status in macrophages from both mouse strains with either single or twice LPS stimulation (Figure 2). The proteins with aerobic respiration and interferon-gamma responses were the groups with the highest fold enrichment in Ezh2 control cells and Ezh2 null macrophages, respectively, after a single LPS activation (Figure 2, left). In LPS tolerance, the proteins with interferon-gamma responses and the negative regulation of innate immune responses were the groups with the highest fold enrichment in Ezh2 control cells and Ezh2 null macrophages, respectively (Figure 2, right). These data implied similar downstream LPS responses in macrophages of both mouse strains. Although there was no direct comparison between Ezh2 control macrophages versus Ezh2 null cells, the Venn diagram analysis, using the Venny 2.1 program (<https://bioinfogp.cnb.csic.es/tools/venny>) accessed on 15 March 2023, from the list of proteins roughly indicated differences in the deviation of the macrophage proteome away from the resting control condition (activated cells versus control cells) (Figure 3). With a single LPS, 307 and 42 proteins were up- or downregulated in macrophages of littermate control mice (LPS Ezh2 control vs. Ezh2 control) and Ezh2 null mice (LPS Ezh2 null vs. Ezh2 null), respectively, with 32 unique proteins presenting only in the latter group (Figure 3, upper). Because the unique proteins in Ezh2 null macrophages might be responsible for the phenotypic differences between Ezh2 null versus Ezh2 control cells after LPS activation, these proteins were further evaluated by the ShinyGO 0.77 program. Interestingly, these 32 proteins were the member of only 2 pathways, including nuclear factor- κ B (NF- κ B) and Toll-like receptor (TLR) pathways (Figure 3, upper). Similarly, after LPS tolerance, 1248 and 1269 proteins were altered from the neutral state (up- or downregulation) in the proteome of macrophages from littermate control mice (Ezh2 control) and Ezh2 null mice, respectively, with 104 unique peptides presenting only in Ezh2 null macrophages (Figure 3, lower) which also were mostly associated with cell energy status and immune responses (Figure 3, lower). Details of the proteins from macrophages uniquely elevated in Ezh2 null cells but not in Ezh2 control macrophages are indicated in Supplementary Tables S1 and S2.

As expected, analysis of the secreted proteins from supernatant (secretome analysis) that deviated from the neutral status demonstrated the lesser proteins (Figure 4) compared with the analysis from the cell lysate (Figure 2). There were 6 and 23 up- and downregulated proteins, respectively, in the secretome of LPS Ezh2 control vs. Ezh2 control and 2 and 22 up- and downregulated proteins, respectively, in the secretome of LPS Ezh2 null vs. Ezh2 null (Figure 4, left). Meanwhile, there were 26 and 66 up- and downregulated proteins, respectively, in the secretome of LPS/LPS Ezh2 control vs. Ezh2 control and 8 and 1 up- and downregulated proteins, respectively, in the secretome of LPS/LPS Ezh2 null vs. Ezh2 null (Figure 4, right). Additionally, The Venn diagram demonstrated 106 and 11 overlapped proteins after the activation compared with the neutral state in the cells from each mouse strain after a single LPS and LPS tolerance, respectively (Figure 5). The fold enrichment pathway analysis of the unique proteins in Ezh2 null macrophages indicated an involvement in cell energy status and responses against infection in a single LPS stimulation (Figure 5, upper), while mostly involved in responses to infection in the LPS tolerance group (Figure 5, lower). Details of the proteins in secretome analysis that were uniquely elevated in Ezh2 null cells but not in Ezh2 control macrophages are indicated in Supplementary Tables S3 and S4. These data implied fewer activities of Ezh2 null macrophages compare with the control cells after activation by either LPS or LPS tolerance that might be responsible for the phenotypic responses against LPS.

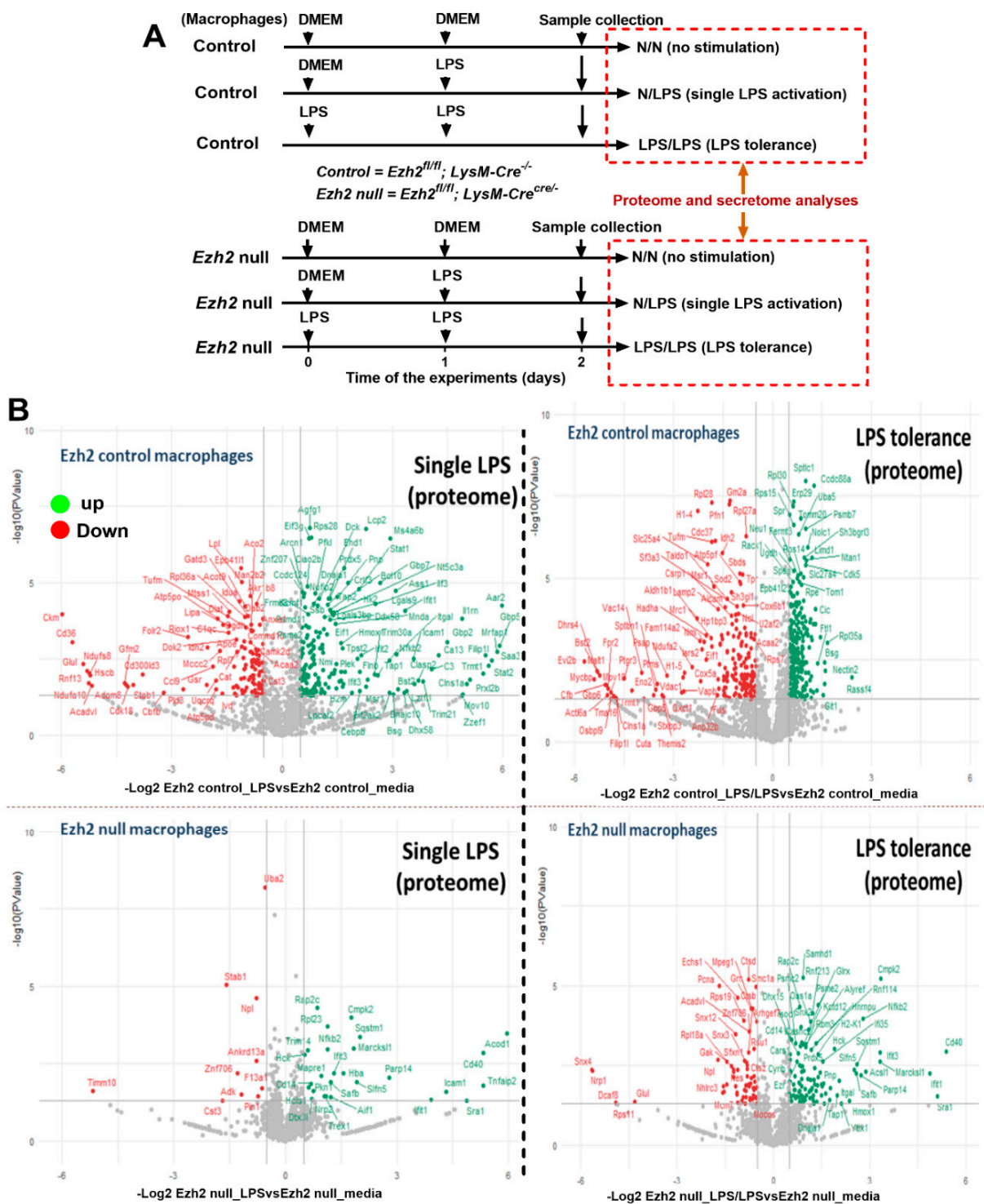


Figure 1. Schema of the experiments using bone marrow-derived macrophages (macrophages) from control mice (*Ezh2^{fl/fl}; LysM-Cre^{-/-}*) or *Ezh2* null mice (*Ezh2^{fl/fl}; LysM-Cre^{cre/-}*) after activation by lipopolysaccharide (LPS) in a single protocol (N/LPS) that started with the culture media (DMEM) followed by LPS 24 h later or LPS tolerance (LPS/LPS) by the repeated LPS stimulations or no stimulation control (N/N) with DMEM incubation (A) is demonstrated. The volcano plot indicating the up- and downregulated proteins, in green and red color, respectively, as compared between the activated cells versus the non-stimulated cells (B) is demonstrated. Macrophages were isolated from 3 different mice for the triplicate analysis.

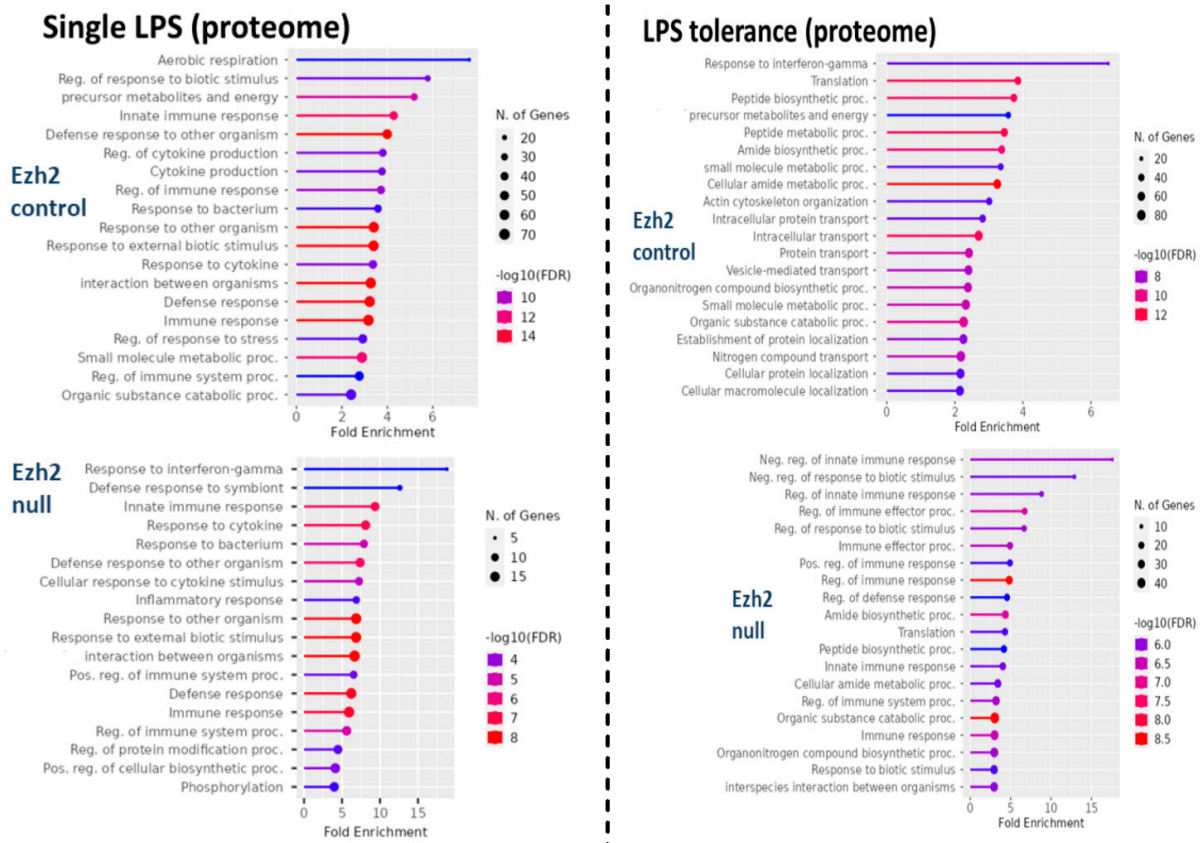


Figure 2. Fold enrichment analysis of cellular proteins in macrophages (proteome) from Ezh2 control (Ezh^{fl/fl}; LysM-Cre^{-/-}) (Ezh2 control) or Ezh2 null mice (Ezh^{fl/fl}; LysM-Cre^{cre/-}) (Ezh2 null) after a single lipopolysaccharide (LPS) activation (left side) or LPS tolerance (right side) between Ezh2 control cells or Ezh2 null macrophages with versus without activation is demonstrated.

2.2. Less Prominent M1 Macrophage Polarization in LPS-Activated Ezh2 Null Cells with the Downregulation of NF- κ B after A Single and Twice LPS Stimulation

Then, macrophages from Ezh2 control (Ezh^{fl/fl}; LysM-Cre^{-/-}) and Ezh2 null (Ezh^{fl/fl}; LysM-Cre^{cre/-}) mice were tested. Here, the supernatant was removed and the cells were washed 1 day post-incubation before the difference between single and twice LPS stimulations was determined at 2 days to control the duration of culture in both groups (Figure 6A). As such, both a single (N/LPS) and LPS tolerance (LPS/LPS) upregulated M1 macrophage polarization compared with control, as determined by supernatant interleukin (IL)-1 β with upregulated IL-1 β and inducible nitric oxide synthase (*iNOS*), without an alteration in genes of M2 polarization, including resistin-like- α (*Retnla* or *Fizz-1*), arginase-1 (*Arg-1*), and transforming growth factor beta (*TGF- β*) (Figure 6B–F). In addition, the characteristic of LPS tolerance, a less potent response to the following LPS stimulations compared with the first response to LPS [55–57] was demonstrated in both control and Ezh2 null cells, as the gene expression of *TNF- α* and *IL-6* (but not *IL-10*) in N/LPS were more prominent than LPS tolerance (Figure 6G–I). However, the expression of genes for pro-inflammatory molecule nuclear factor kappa B (*NF- κ B*) was similarly higher than in the control group (N/N) (Figure 6J). On the other hand, there was a less prominent M1 polarization (pro-inflammatory macrophages), as indicated by *IL-1 β* and *iNOS*, together with less pro-inflammatory responses (*TNF- α* , *IL-6*, and *NF- κ B*) in Ezh2 null macrophages compared with control cells after a single LPS stimulation (N/LPS) (Figure 6C–J) supporting a pro-inflammatory effect of Ezh2 on macrophages [39]. In LPS tolerance (LPS/LPS), there was a non-difference in supernatant IL-1 β , macrophage polarization, and cytokine genes between Ezh2 null macrophages and control cells, despite lower *NF- κ B* expression in Ezh2 null macrophages (Figure 6B–J). Between Ezh2 null macrophages with a single LPS and

LPS tolerance, all of these parameters were similar (Figure 6B–J). Despite lower *NF-κB* (a pro-inflammation molecule) in *Ezh2* null macrophages with LPS tolerance compared with control cells (Figure 6J), supernatant IL-1β (Figure 6B) and expression of cytokine genes (Figure 6G–I) in *Ezh2* null macrophages were similar to that in control cells, implying a limited *Ezh2* impact on the control of macrophage responses during LPS tolerance. Although there was a limited impact on LPS tolerance, these data supported an anti-inflammatory response of *Ezh2* null macrophages after a single LPS stimulation that might be useful as an anti-inflammation in sepsis.

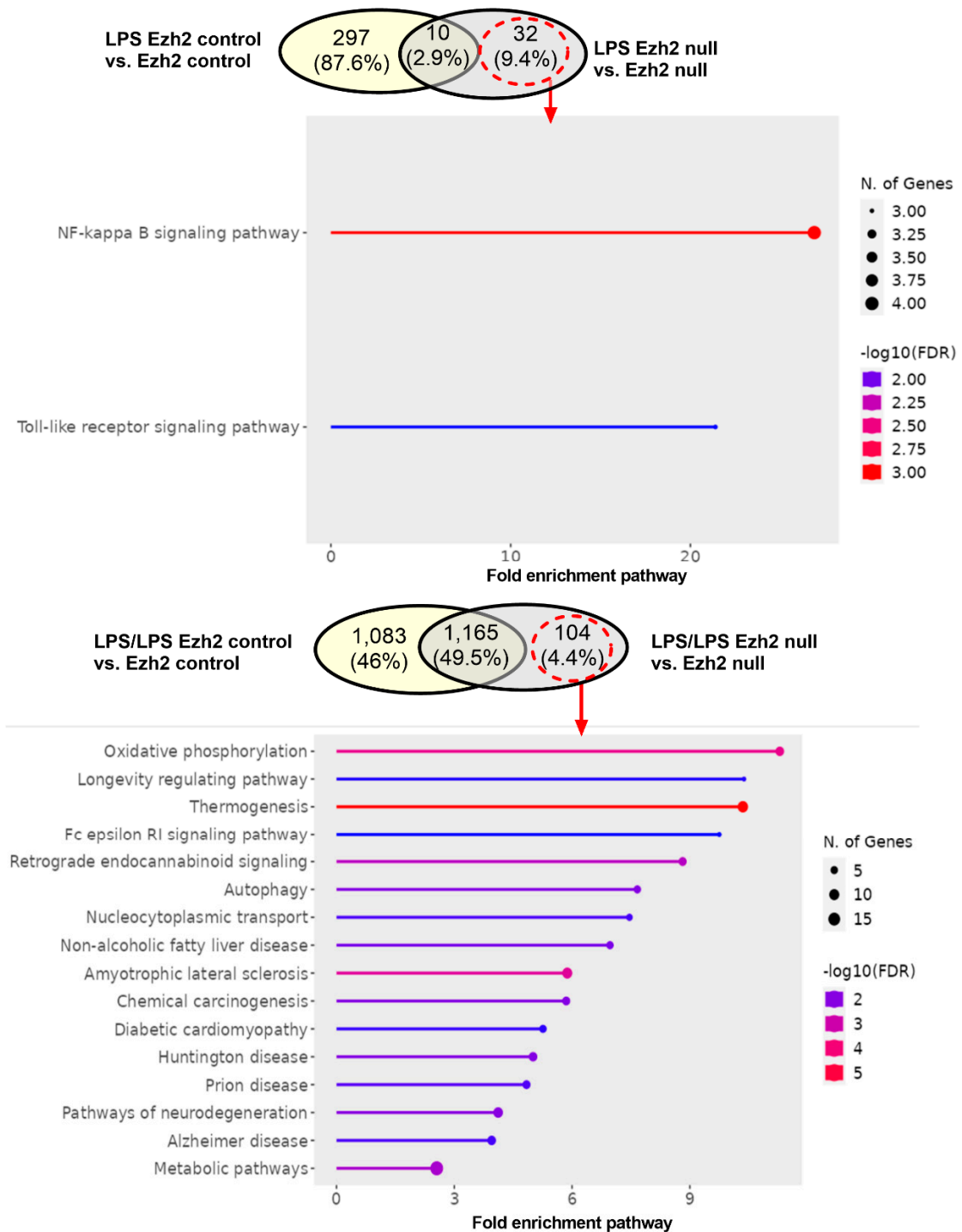


Figure 3. The Venn diagrams of proteome analysis from macrophages of *Ezh2* control (*Ezh2^{fl/fl}*; *LysM-Cre^{-/-}*) (*Ezh2* control) or *Ezh2* null mice (*Ezh2^{fl/fl}*; *LysM-Cre^{cre/-}*) (*Ezh2* null) after a single

lipopolysaccharide (LPS) activation (**upper**) or LPS tolerance (**lower**) between Ezh2 control cells or Ezh2 null macrophages versus the non-activated control of each group are demonstrated. The fold enrichment pathway of the unique proteins that presented only in LPS-stimulated macrophages but not in the Ezh2 control cells (dashed circles with arrows) is also demonstrated. Notably, percentages in the Venn diagram are the number of proteins in each part divided by the total number of proteins from both groups.

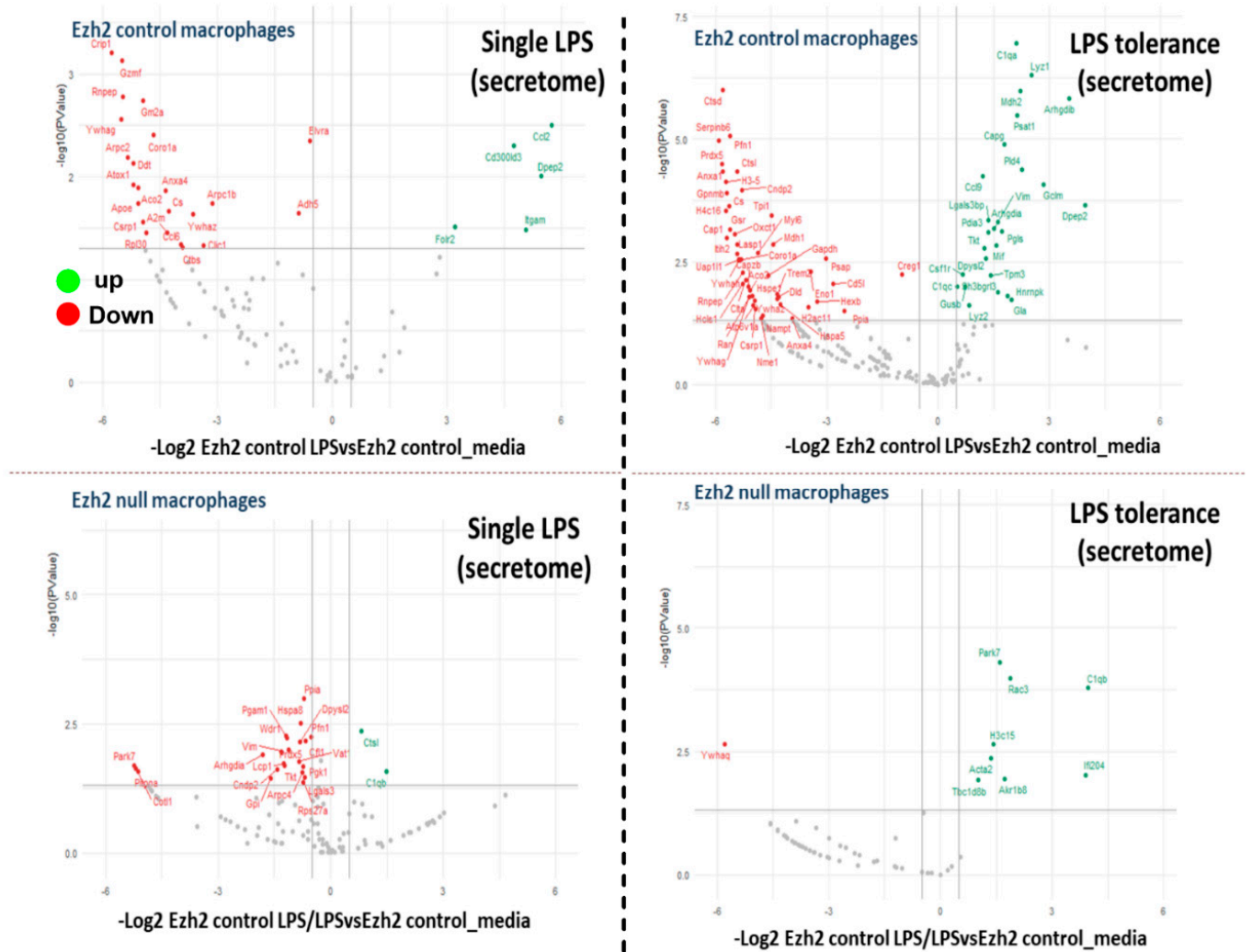


Figure 4. The volcano plots of secretome analysis from macrophages of Ezh2 control (Ezh^{fl/fl}; LysM-Cre^{-/-}) (Ezh2 control) or Ezh2 null mice (Ezh^{fl/fl}; LysM-Cre^{cre/-}) (Ezh2 null) after a single lipopolysaccharide (LPS) activation (**left side**) or LPS tolerance (**right side**) between Ezh2 control cells (**upper**) or Ezh2 null macrophages (**lower**) with versus without the activations are demonstrated.



Figure 5. The Venn diagrams of secretome analysis from macrophages of Ezh2 control (Ezh^{fl/fl}; LysM-Cre^{-/-}) (Ezh2 control) or Ezh2 null mice (Ezh^{fl/fl}; LysM-Cre^{cre/-}) (Ezh2 null) after a single lipopolysaccharide (LPS) activation (**upper**) or LPS tolerance (**lower**) between Ezh2 control cells or Ezh2 null macrophages versus the non-activated control of each group are demonstrated. The fold enrichment pathway of the unique proteins that presented only in LPS-stimulated macrophages but not in the Ezh2 control cells (dashed circles with arrows) is also demonstrated. Notably, percentages in the Venn diagram are the number of proteins in each part divided by the total number of proteins from both groups.

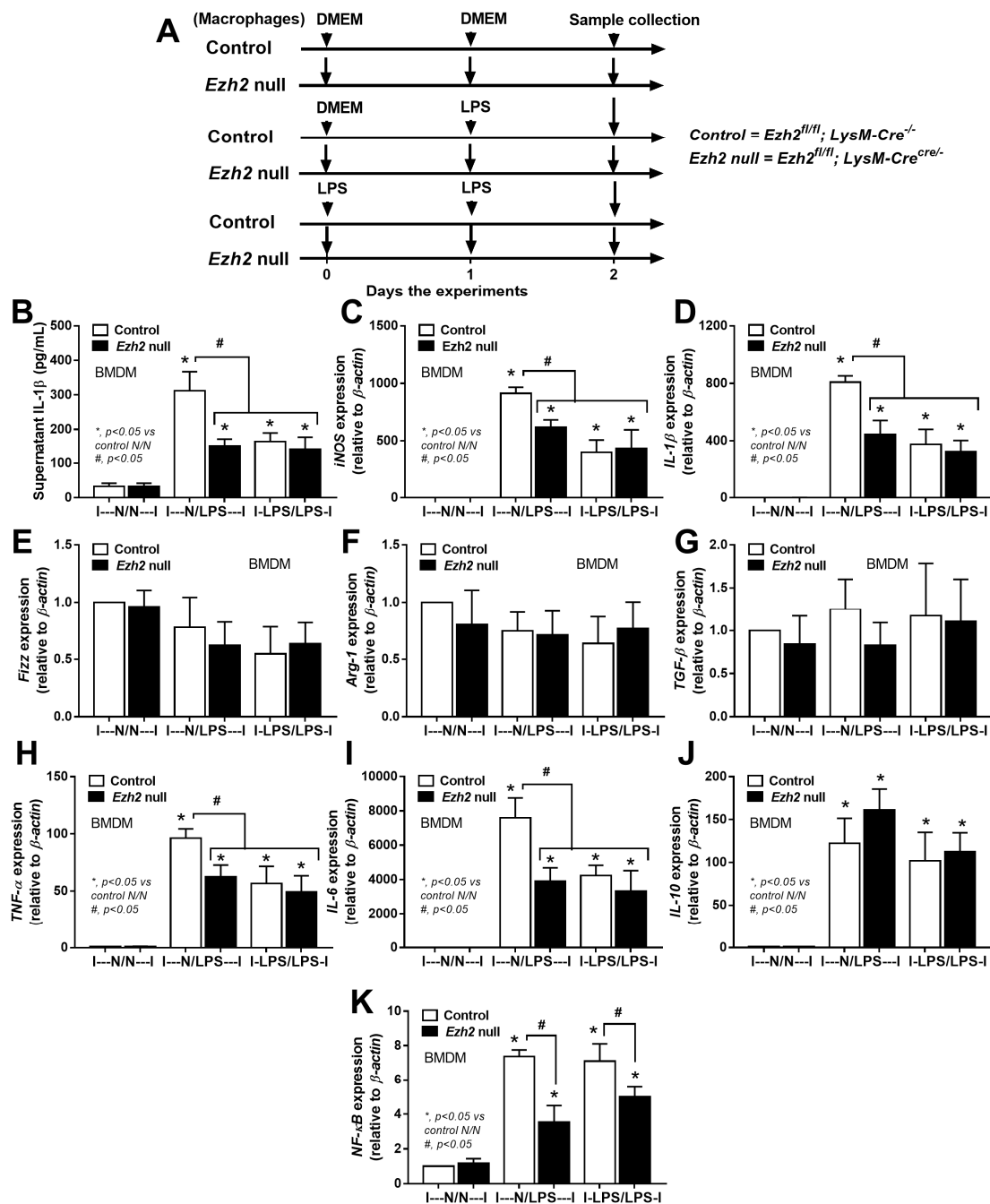


Figure 6. The schema of the experiments in bone marrow-derived macrophages (BMDM) from *Ezh2* control (*Ezh2^{fl/fl}; LysM-Cre^{-/-}*) or *Ezh2* null (*Ezh2^{fl/fl}; LysM-Cre^{cre/-}*) mice after activation by lipopolysaccharide (LPS) in a single protocol (N/LPS) that started with the culture media followed by LPS at 24 h later or LPS tolerance (LPS/LPS) by the twice LPS stimulations or control (N/N) using the twice culture media incubation (A) is demonstrated. The characteristics of these macrophages with different protocols, as indicated by supernatant IL-1 β (B) with the expression of genes for M1 macrophage polarization (*IL-1 β* and *iNOS*) and M2 polarization (*Fizz-1*, *Arg-1*, and *TGF- β*) (C–G), inflammatory genes (*TNF- α* , *IL-6*, and *IL-10*) (H–J), and inflammatory mediators (*NF- κ B*) (K) are demonstrated. Triplicated independent experiments were performed. Mean \pm SEM is presented with the one-way ANOVA followed by Tukey’s analysis (*, $p < 0.05$ vs. WT N/N and #, $p < 0.05$).

2.3. Characteristics of Ezh2 Control ($Ezh2^{fl/fl}; LysM-Cre^{-/-}$) or Ezh2 Null ($Ezh2^{fl/fl}; LysM-Cre^{cre/-}$) Mice after Cecal Ligation and Puncture (CLP) and LPS Tolerance before CLP Surgery

To investigate the impact of Ezh2 in macrophages on hyper-inflammatory sepsis and sepsis after LPS tolerance, CLP after PBS injection (CLP) and CLP after twice LPS administration (LPS-CLP), respectively, in Ezh2 control ($Ezh2^{fl/fl}; LysM-Cre^{-/-}$) and Ezh2 null ($Ezh2^{fl/fl}; LysM-Cre^{cre/-}$) mice was performed (Figure 7A). In the survival analysis, CLP after LPS tolerance (LPS-CLP) in control mice showed the most severe sepsis as all mice died within 72 h post-surgery (Figure 7A). The more severe sepsis in LPS-CLP mice compared with CLP, especially in the control mice (Figure 7A), implied a possible impact of LPS tolerance on a defect of microbial control. Interestingly, the best survival rate of Ezh2 null mice with CLP and the better survival rate after LPS-CLP of Ezh2 null compared with control mice (Figure 7A) indicated a possible beneficial impact of Ezh2 blockage in macrophages during sepsis. Among the control group, LPS-CLP demonstrated more severe sepsis than CLP alone as indicated by cell-free DNA, bacteremia, and pro-inflammatory cytokines (TNF- α and IL-6), but not other parameters (serum creatinine, alanine transaminase, renal histology score, spleen apoptosis, endotoxemia, and IL-10) (Figures 7C–L and 8). These data indicated more severe sepsis after LPS tolerance compared with no LPS tolerance in the Ezh2 control mice, possibly due to immune exhaustion. However, there was no difference in most of the sepsis severity biomarkers between Ezh2 null mice with LPS-CLP and those with CLP alone, except the higher histology score in LPS-CLP Ezh2 null mice (Figure 7C–L). The data implied no or less immune exhaustion after LPS tolerance in Ezh2 null mice, as mentioned in previous publications [39,58]. Between Ezh2 null versus Ezh2 control mice with CLP-induced sepsis hyperinflammation (CLP) and LPS tolerance with subsequent sepsis (LPS-CLP), sepsis severity was more severe in Ezh2 control mice as indicated by survival analysis, organ injury (kidney and liver), cell-free DNA, endotoxemia, bacteremia, and serum cytokines (TNF- α and IL-6, but not IL-10) (Figure 7C–L), supporting a beneficial impact of Ezh2 deletion in macrophages during sepsis in both conditions.

2.4. Ezh2 Inhibitor Attenuated Cecal Ligation and Puncture (CLP) Sepsis in Wild-Type (WT) Mice with Less Impact on CLP after LPS Tolerance

Due to the reduced sepsis severity of Ezh2 null over Ezh2 control mice from our data and the control of inhibitory Socs3 by Ezh2 gene from previous publications [59,60], an Ezh2 inhibitor was further tested, similar to the experiments on Ezh2 null mice mentioned above (Figure 9A). In WT mice, CLP after LPS tolerance (LPS-CLP) also demonstrated the highest mortality rate as all mice died within 96 h of the observation, while approximately 25% of the mice survived at 96 h post-surgery with CLP alone (Figure 9B), supporting more severe sepsis after LPS tolerance similar to Ezh2 control mice (Figure 7A–L). However, Ezh2 inhibitor attenuated disease severity only in CLP alone, but not LPS-CLP (Figure 9B), perhaps because of the more severe sepsis in LPS-CLP compared with CLP alone, as indicated by higher cell-free DNA and serum cytokines (TNF- α and IL-6) in vehicle-administered LPS-CLP mice compared with the CLP alone group (Figure 9E,H,I). In CLP alone, the Ezh2 inhibitor attenuated kidney damage (serum creatinine) and serum cytokines (TNF- α , IL-6, and IL-10) but not cell-free DNA, endotoxemia, and bacteremia (Figure 9B–J). On the other hand, the Ezh2 inhibitor did not attenuate LPS-CLP mice, as indicated by the non-difference in survival analysis, organ damage (kidney and liver), endotoxemia, and bacteremia (Figure 9B–D,F,G), despite the reduction of cell-free DNA and serum cytokines (TNF- α , IL-6, and IL-10) in Ezh2 inhibitor-administered mice (Figure 9E,H–J).

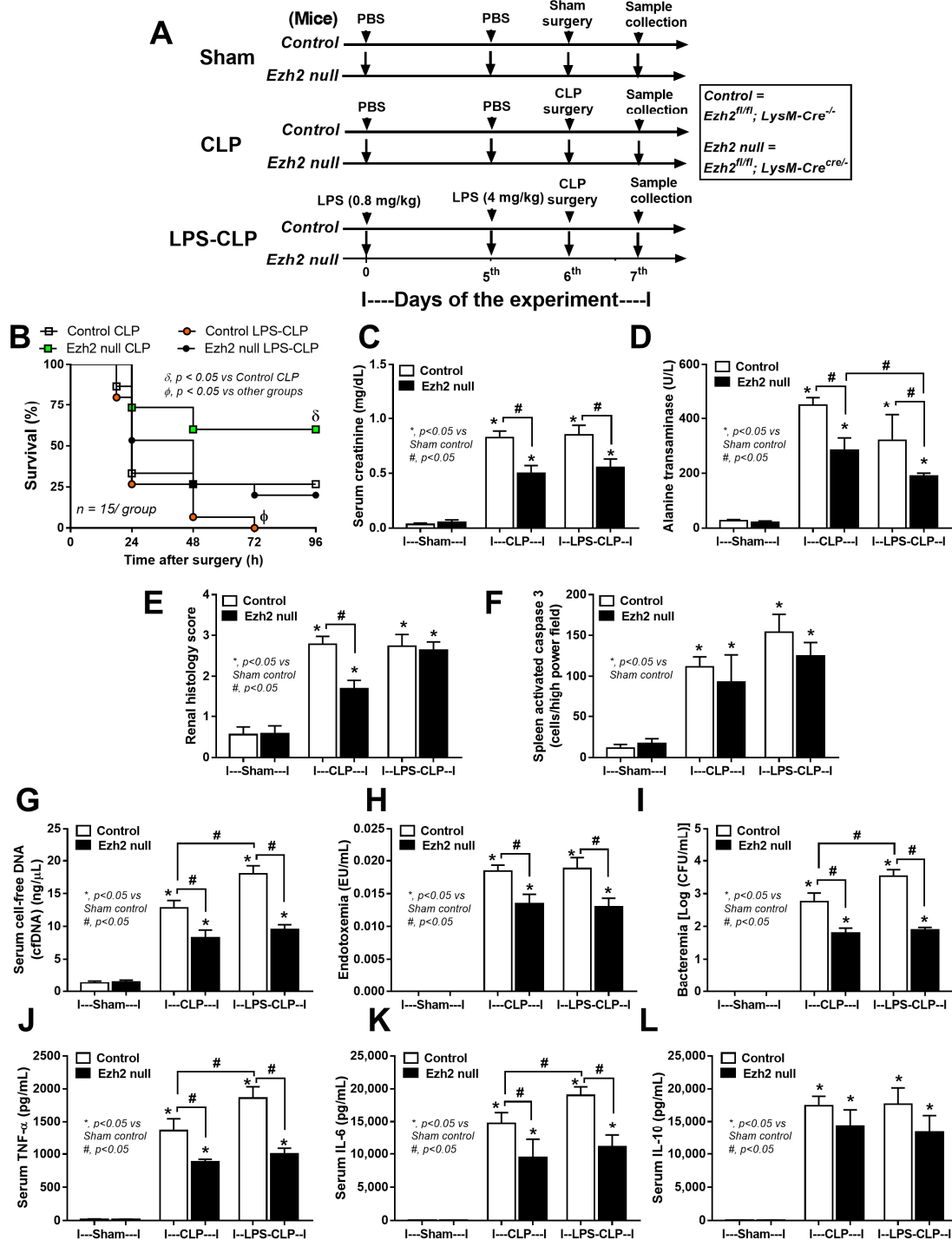


Figure 7. The schema of the experiments in Ezh2 control ($Ezh2^{fl/fl}; LysM-Cre^{-/-}$) (Control) or Ezh2 null ($Ezh2^{fl/fl}; LysM-Cre^{cre/-}$) mice (Ezh2 null) in sham, cecal ligation and puncture surgery (CLP), and lipopolysaccharide (LPS) tolerance before CLP surgery (LPS-CLP). The protocol start by injection of phosphate buffer solution (PBS) or LPS intraperitoneal (ip) injection (0.8 mg/kg) followed by PBS or LPS (ip 4 mg/kg) at 5th day before sham or CLP surgery at 6th day, and sacrifice with sample collection at 7th day of the experiment (A). Characteristics of these mice as indicated by survival analysis (B), kidney injury (serum creatinine) (C), liver damage (alanine transaminase) (D), renal injury score (E), spleen apoptosis (F), cell-free DNA (G), endotoxemia (H), bacteremia (I), and serum cytokines (TNF- α , IL-6, and IL-10) (J–L) are demonstrated ($n = 15$ /group for B and $n = 5-7$ /group for (C–J)). Mean \pm SEM is presented with the one-way ANOVA followed by Tukey’s analysis (*, $p < 0.05$ vs. Sham control and #, $p < 0.05$).

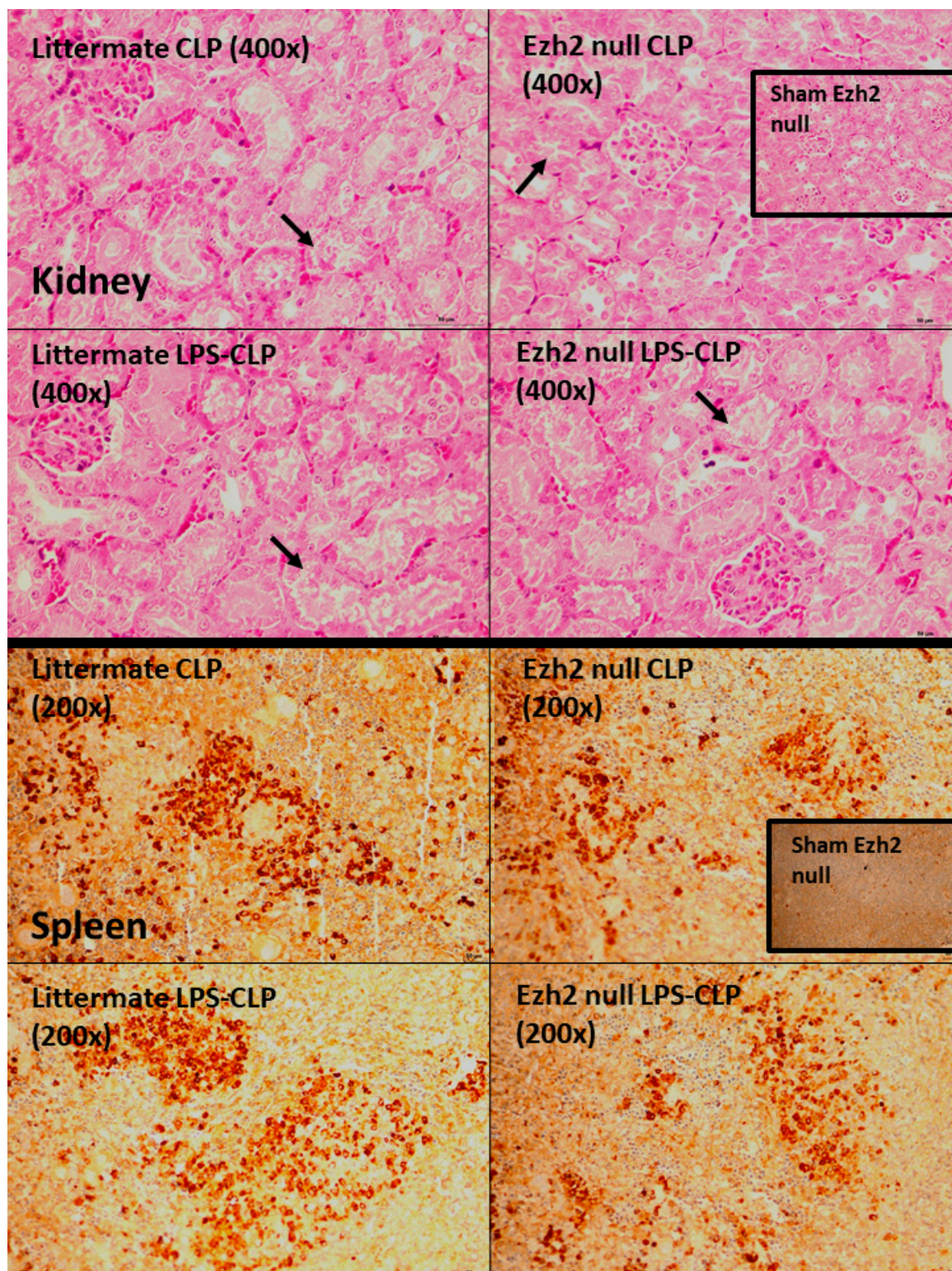


Figure 8. Representative pictures of renal histology with hematoxylin and eosin (H&E) stain (**upper**) and activated caspase 3 spleen apoptosis (**lower**) of Ezh2 control ($Ezh^{fl/fl}; LysM-Cre^{-/-}$) (littermate) or Ezh2 null ($Ezh^{fl/fl}; LysM-Cre^{cre/-}$) mice (Ezh2 null) in cecal ligation and puncture surgery (CLP), and lipopolysaccharide (LPS) tolerance before CLP surgery (LPS-CLP) are shown. Only the sham of Ezh2 null mice, but not the sham of littermate control, in renal histology and spleen apoptosis are demonstrated in the inset pictures due to the non-difference between both shams. Arrows indicate an example of renal tubular cell injury.

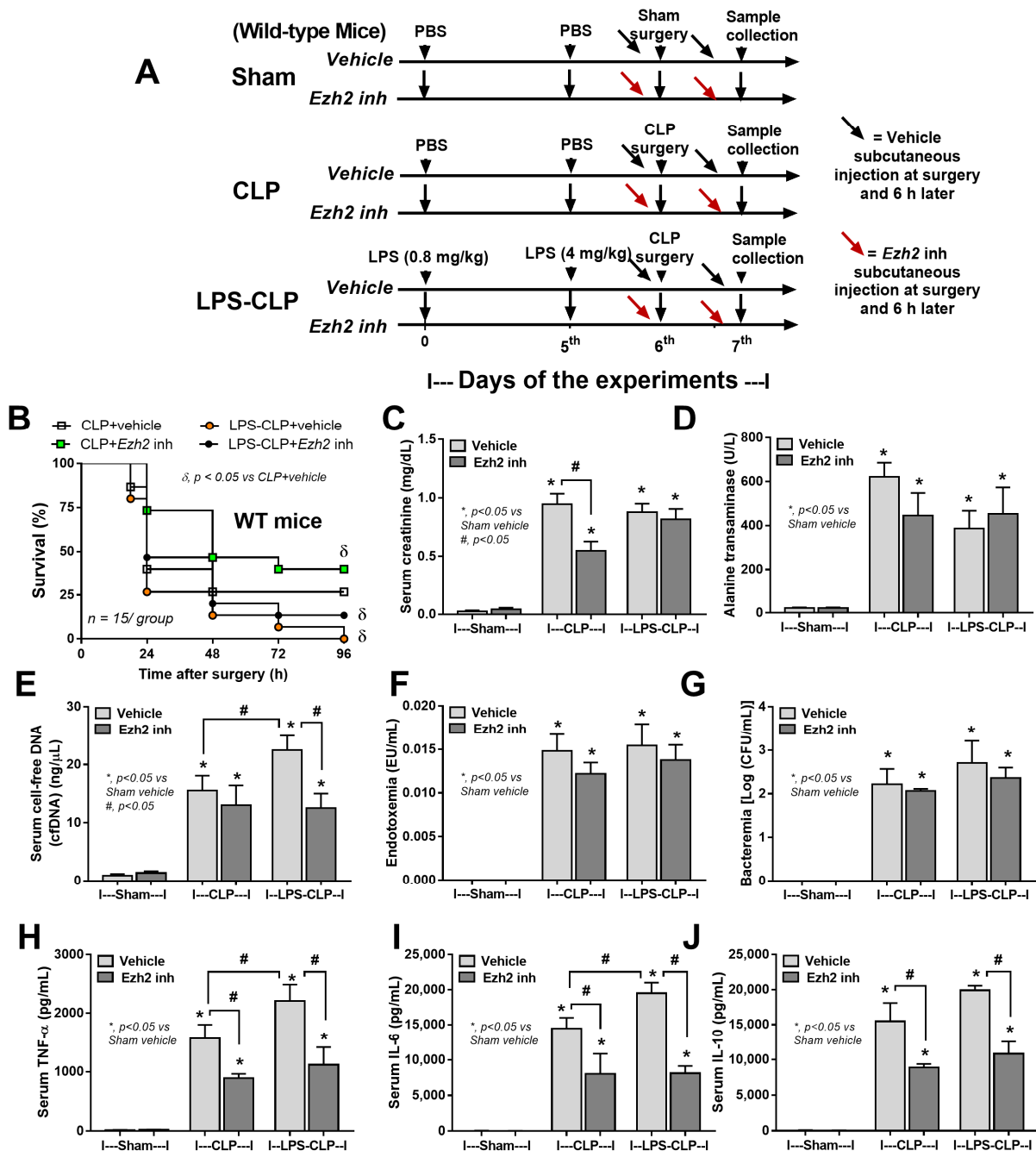


Figure 9. The schema of the experiments in wild-type mice in sham, cecal ligation and puncture surgery (CLP), and lipopolysaccharide (LPS) tolerance before CLP surgery (LPS-CLP). The protocol start by injection of phosphate buffer solution (PBS) or LPS intraperitoneal (ip) injection (0.8 mg/kg) followed by PBS or LPS (ip 4 mg/kg) at 5th day before sham or CLP surgery at 6th day, and sacrifice with sample collection at 7th day of the experiment. Mice were subcutaneously administered with vehicle or an Ezh2 inhibitor at 0 and 6 h post-surgery on the 6th day of protocol (A). Characteristics of these mice as indicated by survival analysis (B), kidney injury (serum creatinine) (C), liver damage (alanine transaminase) (D), cell-free DNA (E), endotoxemia (F), bacteremia (G), and serum cytokines (TNF- α , IL-6, and IL-10) (H–J) are demonstrated ($n = 15/\text{group}$ for B and $n = 5\text{--}7/\text{group}$ for (C–J)). Mean \pm SEM is presented with the one-way ANOVA followed by Tukey’s analysis ($*$, $p < 0.05$ vs. Sham vehicle control and $\#$, $p < 0.05$).

3. Discussion

Lipopolysaccharide (LPS) is one of the potent activators of macrophages, as indicated by the up- and downregulation of several proteins compared with the neutral state of the cells. The macrophages from Ezh2 littermate control or Ezh2 null mice without activation were used as the controls to see the deviation away from the neutral state due to the possible differences between littermate control and Ezh2 null mice. Less profound activities of Ezh2 null macrophages were indicated by a lower number of proteins with similar functions (immune responses, cytokines, and cell energy) between control and Ezh2 null cells, implying similar downstream signals. Because of (i) the possibly reduced adverse effects of selective inhibition only on macrophages but not all cells in the body [61], (ii) endotoxemia in several conditions [62–64], partly through gut barrier damage [1,22,24,26] with profound LPS recognition by macrophages [65,66] and (iii) the epigenetic regulation in LPS responses [67], LPS was used to test Ezh2 null macrophages. Notably, Ezh2 reduced chromatin accessibility by adding methyl marks at the tail of histone H3, and the presence of trimethylation of H3K27 (H3K27me3) at promoter regions [68] is mentioned in sepsis [69]. Indeed, the increased mortality in patients with high *Ezh2* and H3K27 is mentioned [70,71] and inhibition of Ezh2 [72] might be beneficial. M1 macrophage polarization (*IL-1 β* and *iNOS*) along with pro-inflammatory molecules (*TNF- α* , *IL-6*, and *NF- κ B*) were less prominent in LPS-activated Ezh2 null macrophages than the control (Figure 6), possibly correlated with more profound suppressor of cytokine signaling 3 (*Socs3*; an anti-inflammatory molecule) as mentioned in our previous publication [39]. Perhaps *Ezh2* more potently inhibits some molecules than others. In a single LPS stimulation, Ezh2 more profoundly suppressed *Socs3* than *NF- κ B* (a transcriptional factor for several cytokines), resulting in less inhibition of *NF- κ B* with high cytokine production. Without Ezh2, elevated *Socs3* downregulated *NF- κ B* and led to lower *TNF- α* and *IL-6* expression after a single LPS stimulation. Indeed, cytosolic *Socs3* inhibits the *NF- κ B*-dependent inflammatory genes through enhanced ubiquitination and proteasomal degradation [44,59]. Additionally, Ezh2 blockage enhances anti-inflammatory *Socs3* that inhibits hyperinflammation in sepsis (here and others), multiple sclerosis, and glucose-activated peritoneal fibrosis [60,69,73]. In contrast, suppression of Ezh2 might enhance pro-inflammatory genes, including *NF- κ B*, that possibly worsens inflammatory bowel diseases and muscle cell apoptosis in sepsis [49,74–76]. Although *Socs3* can inhibit both anti- and pro-inflammatory cytokines [77], possibly driven by different molecules [78], *Socs3* seems to have less impact on anti-inflammatory IL-10 as serum *TNF- α* and *IL-6*, but not IL-10, were lower in LPS-injected Ezh2 null mice [39]. Accordingly, *Socs3* might be correlated with IL-10 in macrophages responses because (i) IL-10 directly upregulates *Socs3* [79], (ii) *Socs3* and IL-10 are simultaneously used to inhibit inflammation [80,81], and (iii) Ezh2 inhibitor (EPZ-6438) upregulated *IL-10* [82].

In mice, the deletion of Ezh2 only in myeloid cells in Ezh2 null mice was enough to induce less severe sepsis, similar to the LPS injection model [39] and pneumococcal sepsis model [70,83], highlighting the major impact of macrophages in the cytokine production [84]. Then, blockage of cytokine production only on the myeloid cells, especially macrophages, might be beneficial. Despite the improved sepsis mortality with the previously known hepatic protection of Ezh2 inhibitor [85], liver enzyme and bacteremia were not different from sepsis in Ezh2 control mice (Figure 7) implying a possible hepatotoxicity and incomplete Ezh2 blockage of the selected inhibitor (GSK126). Notably, injection of Ezh2 inhibitor [86] in mice inhibits Ezh2 in all cells which might be harmful in some cell types and the selective Ezh2 blockage only in macrophages might reduce the adverse effect. However, the balance between the pro- and anti-inflammatory directions (a yin–yang effect) after Ezh2 blockage might be different in individual patients.

Because leaky gut causes endotoxemia [1,66] and relatively low inflammation (repeat or chronic exposure of LPS), or LPS tolerance [24,87] possibly causes more severe sepsis [25] and/or secondary infection [31,88,89], CLP surgery after LPS tolerance (LPS-CLP) might be different from CLP without LPS priming (CLP). In control mice, LPS-CLP was more severe than in those with CLP alone, possibly due to inadequate inflammation to control

organisms at an early phase of sepsis [25] leading to a higher blood bacterial burden and higher cytokines than in the CLP alone group. Because chronic endotoxemia might induce LPS tolerance [25,57], sepsis in these individuals, such as obesity and uremia, might be more severe than the non-endotoxemia cases [90–95], partly, due to LPS tolerance. Despite the higher disease severity of LPS-CLP over CLP alone, *Ezh2* null mice still demonstrated less severe sepsis compared with LPS-CLP in control mice, supporting the anti-inflammatory effect of *Ezh2* deletion in macrophages. Although the *Ezh2* inhibitor did not reduce LPS-CLP mortality, there was less severe systemic inflammation, implying a possible benefit of the dose adjustment. More studies are interesting. Despite the broad spectrum antiviral of *Ezh1/2* inhibitors [96], the influence of *Ezh1/2* blockage on bacterial infection needs further testing. In cancer, *Ezh2* blockage might induce anti-inflammatory macrophages, resulting in less severe sepsis or more infection susceptibility due to the inadequate inflammation to control organisms. Importantly, an effective antibiotic with good microbial control is a main strategy for the treatment of sepsis-induced hyper-inflammation [97]. Hence, our results are a proof of concept to use clinically available *Ezh2* inhibitors in sepsis, especially the blockage of *Ezh2* specifically only in macrophages.

Several limitations should be mentioned. First, only male mice were used and the impact of gender differences in sepsis might affect the translation of the results. Second, details of mechanistic pathways, including the Western blot analysis, were not performed. Despite a proof of concept for the translational use of *Ezh2* inhibitors in clinical sepsis, more experiments would be interesting. Third, the results need to be validated in human situations before a solid conclusion. Nevertheless, we concluded that *Ezh2* inhibitors, an available anticancer treatment, might be beneficial in some situations of sepsis. More studies are warranted.

4. Materials and Methods

4.1. Animal

The Institutional Animal Care and Use Committee of the Faculty of Medicine, Chulalongkorn University, Bangkok, Thailand approved the protocol (No. 017/2562) according to the National Institutes of Health (NIH) criteria. Wild-type (WT) 8-week-old C57BL/6 male mice were purchased from Nomura Siam, Pathumwan, Bangkok, Thailand. Meanwhile, *Ezh2*^{flox/flox} and *LysM-Cre*^{Cre/Cre} mice were obtained from RIKEN BRC Experimental Animal Division (Ibaraki, Japan) and cross-bred until having *Ezh2* littermate control (*Ezh*^{fl/fl}; *LysM-Cre*^{-/-}) or *Ezh2* null (*Ezh*^{fl/fl}; *LysM-Cre*^{Cre/-}) in F3 generation of the breeding protocol. As such, the *Ezh2*^{flox/flox} mice had loxP sites upstream and downstream of the 2.7 kb SET domain, while bred with *LysM-Cre*^{Cre/Cre} mice, the mice with a Cre recombinase under the control of lysozyme M to target *Ezh2* for deletion in myeloid cells (macrophages and neutrophils). Mice with *Ezh2*^{flox/flox} without *LysM-Cre* (*Ezh*^{fl/fl}; *LysM-Cre*^{-/-}) were used as littermate controls (*Ezh2* control). To genotype these mice on the loxP sites' insertion, the following primers were used for *Ezh2*: reverse 1: 3' of loxP: 5'-AGG GCA TCA GCC TGG CTGTA-3'; forward 2: 5' of loxP: 5'-TTA TTC ATA GAG CCA CCTGG-3'; forward 3: left loxP: 5'-ACG AAA CAG CTC CAG ATTCAG GG-3' according to a previous publication [83]. The mice homozygous for the flox were selected and genotyped for the expression of *LysM-Cre* using the primers; forward: 5'-CTTGGGCTGCCAGAATTCTC-3'; Reverse: 5'-CCCAGAAATGCCAGATTACG-3'.

4.2. Animal Models

Cecal ligation and puncture (CLP) surgery was used to induce sepsis, following previous publications, under isoflurane anesthesia [98–100]. Briefly, a median abdominal incision was performed and the cecum was ligated at 10 cm from the cecal tip, punctured twice with a 21-gauge needle, and gently squeezed to express a small amount of fecal material before closing the abdominal wall layer by layer with sutures. Then, tramadol (25 mg/kg/dose) in 0.25 mL prewarmed normal saline solution (NSS) and imipenem/cilastatin (14 mg/kg/dose) in 0.2 mL NSS were subcutaneously administered

in abdominal areas after surgery, and at 6 and 18 h post-CLP [9]. In sham-operated mice, the cecum was isolated and closed by suturing without ligation or puncture. In parallel, a sham operation was performed with only cecal identification before closing abdomen layer by layer. Because lipopolysaccharide (LPS) tolerance inhibits macrophage cell respiration and induces global proteomic changes in macrophages [35], sepsis during LPS tolerance might be different from the regular condition. Then, CLP after LPS tolerance using twice-administered LPS injection (LPS-CLP) was conducted. Hence, the mice were divided into 3 groups. First, for CLP in LPS tolerance (LPS-CLP), intraperitoneal injection of 0.8 mg/kg LPS (*Escherichia coli* 026:B6) (Sigma-Aldrich, St. Louis, MO, USA) with another dose of 4 mg/kg LPS at 5 days later and followed by CLP surgery at 1 days after the 2nd dose of LPS was performed. Second, for CLP alone (CLP), the experiments started with intraperitoneal injection of phosphate buffer solution (PBS) at 0 and 5 days followed by CLP surgery. Third, in sham control mice (Sham), 2 doses of PBS at 0 and 5th days of experiments followed by sham surgery was conducted. Of note, the lower 1st dose (0.8 mg/kg) followed by the higher 2nd LPS dose (4 mg/kg) for LPS tolerance induction was performed according to a previous protocol [25]. Mice were sacrificed with cardiac puncture under isoflurane anesthesia with sample collection at 24 h or 96 h post-surgery for blood biomarkers and survival analysis, respectively. On the other hand, these mouse protocols, including CLP, LPS-CLP, and sham, were also used for the test of Ezh2 inhibitor using WT mice in all groups. The Ezh2 inhibitor (GSK343; Medchemexpress, Monmouth, NJ, USA) at 4 mM/25 g mice in 3% dimethyl sulfoxide (DMSO) or DMSO alone (vehicle control) was subcutaneously administered 15 min before surgery and 6 h later (15 min before tramadol and the antibiotics). These mice were sacrificed with the same protocol of experiments in the transgenic mice.

4.3. Mouse Sample Analysis

Serum creatinine and alanine transaminase [40] were measured by colorimetric method (QuantiChrom™ Creatinine Assay Kit, BioAssay System, Hayward, CA, USA) and Enzy-Chrom Alanine Transaminase assay (EALT-100, BioAssay), respectively. Serum cell-free DNA and LPS (endotoxin) were detected by Quanti PicoGreen assay (Sigma-Aldrich) and HEK-Blue LPS Detection Kit 2 (InvivoGen™, San Diego, CA, USA), while ELISA (Invitrogen, Carlsbad, CA, USA) was used for detection of cytokines (TNF- α , IL-6, and IL-10). In parallel, blood bacterial abundance (bacteremia) was evaluated using the direct spread of mouse blood onto blood agar plates (Oxoid, Hampshire, UK) in serial dilutions and incubating at 37 °C for 24 h before colony enumeration. For the kidney injury score, the injury score was semi-quantitatively evaluated on hematoxylin and eosin (H&E) staining in 4 mm thick paraffin-embedded slides at 200 \times magnification by the area of injury (tubular epithelial swelling, loss of brush border, vacuolar degeneration, necrotic tubules, cast formation, and desquamation) using the following score: 0, area < 5%; 1, area 5–10%; 2, area 10–25%; 3, area 25–50%; 4, area > 50% [23]. In parallel, for spleen apoptosis, spleens with 10% formalin fixation were stained by anti-active caspase 3 antibody (Cell Signaling Technology, Beverly, MA, USA), using immunohistochemistry, and expressed in positive cells per high-power field (200 \times magnification) as previously published [23].

4.4. Bone Marrow-Derived Macrophages and the In Vitro Experiments

Bone marrow-derived macrophages from mouse femurs using supplemented Dulbecco's Modified Eagle's Medium (DMEM) with conditioned medium of the L929 cells (ATCC CCL-1) were derived as previously described [65,101–103]. The macrophages at 5×10^4 cells/well in supplemented DMEM (Thermo Fisher Scientific, Waltham, MA, USA) were incubated in 5% carbon dioxide (CO₂) at 37 °C for 24 h before being treated by 3 different protocols, including (i) a single LPS stimulation; started with DMEM followed by LPS (100 ng/mL) 24 h later (N/LPS), or (ii) LPS tolerance; using the twice stimulations by 100 ng/mL of LPS (LPS/LPS), or control (N/N) using the twice DMEM incubation, before the sample collection (supernatant and cells). Notably, the supernatant of the

stimulated cells in all groups was gently removed and washed with DMEM before the re-administration of LPS or DMEM, as previously mentioned [39,87,104]. Supernatant interleukin (IL)-1 β was evaluated by ELISA (Invitrogen, Carlsbad, CA, USA) and the gene expression was evaluated by quantitative real-time polymerase chain reaction (PCR), as previously described [102,105–107]. Briefly, the RNA was extracted from the cells with TRIzol Reagent (Invitrogen, Carlsbad, CA, USA) together with RNeasy Mini Kit (Qiagen, Hilden, Germany) as 1 mg of total RNA was used for cDNA synthesis with iScript reverse transcription supermix (Bio-Rad, Hercules, CA, USA). Quantitative real-time PCR was performed on a QuantStudio 6 real-time PCR system (Thermo Fisher Scientific, Waltham, MA, USA) using SsoAdvance Universal SYBR Green Supermix (Bio-Rad, Hercules, CA, USA). Expression values were normalized to beta-actin (β -actin) as an endogenous housekeeping gene and the fold change was calculated by the $\Delta\Delta C_t$ method. The primers used in this study are listed in Table 1.

Table 1. List of primers used in the study.

| Name | Forward | Reverse |
|-----------------------------------------------------------------------------------------|--------------------------------|---------------------------------|
| Inducible nitric oxide synthase (<i>iNOS</i>); Gene ID: 18126 | 5'-ACCCACATCTGGCAGAATGAG-3' | 5'-AGCCATGACCTTTTCGCATTAG-3' |
| Interleukin-1 β (<i>IL-1β</i>) Gene ID: 16176 | 5'-GAAATGCCACCTTTTGACAGTG-3' | 5'-TGGATGCTCTCATCAGGACAG-3' |
| Tumor necrosis factor α (<i>TNF-α</i>) Gene ID: 21926 | 5'-CCTCACACTCAGATCATCTTCTC-3' | 5'-AGATCCATGCCGTTGGCCAG-3' |
| Interleukin-6 (<i>IL-6</i>) Gene ID: 16193 | 5'-TACCACTTCACAAGTCGGAGGC-3' | 5'-CTGCAAGTGCA TCA TCGTTGTTC-3' |
| Interleukin-10 (<i>IL-10</i>) Gene ID: 16153 | 5'-GCTCTTACTGACTGGCATGAG-3' | 5'-CGCAGCTCTAGGAGCATGTG-3' |
| Arginase-1 (<i>Arg-1</i>) Gene ID: 11846 | 5'-CTTGGCTTGCTTCGGAAGTC-3' | 5'-GGAGAAGGCGTTTGCTTAGTT-3' |
| Resistin-like molecule- α 1 (<i>FIZZ-1</i>) Gene ID: 57262 | 5'-GCCAGGTCCTGGAACCTTTC-3' | 5'-GGAGCAGGGAGATGCAGATGA-3' |
| Transforming growth factor- β (<i>TGF-β</i>) Gene ID: 21813 | 5'-CAGAGCTGCGCTTGCAGAG-3' | 5'-GTCAGCAGCCGTTACCAAG-3' |
| Nuclear factor kappa B (<i>NFκB</i>) Gene ID: 18033 | 5'-CTTCCTCAGCCATGGTACCTCT-3' | 5'-CAAGTCTTCATCAGCATCAAAGT-3' |
| β -actin Gene ID: 11461 | 5'-CGGTTCCGATGCCCTGAGGCTCTT-3' | 5'-CGTCACACTTCATGATGGAATTGA-3' |

4.5. Mass Spectrometry Proteomic and Secretome Analysis

The proteomic and secretome analyses were performed, using the cells and supernatant media, respectively, according to previous publications [35,56,104]. Briefly, for proteome analysis, the activated macrophages (1×10^6 cells/well) with 3 protocols, N/N, N/LPS, and LPS/LPS as mentioned above, were processed for in-solution digestion. For secretome analysis, an equal volume of culture medium from 3 conditions was centrifuged to remove intact cells, concentrated by centrifugation in an Amicon Ultracel—3K (EMD Millipore, Billerica, MA, USA), and the buffer exchanged using 8 M urea lysis buffer. The concentrated proteins were also subjected to in-solution digestion. Then, the peptides from N/N, N/LPS, and LPS/LPS from the cells and culture media samples, for proteome and secretome, respectively, were labeled with light reagents (CH₂O and NaBH₃CN), medium reagents (CD₂O and NaBH₃CN), and heavy reagents (13CD₂O and NaBD₃CN), respectively. The pooled peptides were fractionated using a high pH reversed-phase peptide fractionation kit (Thermo Fisher Scientific, San Jose, CA, USA). Liquid chromatography–tandem mass spectrometry (LC-MS/MS) analysis of samples was performed on an EASY-nLC1000 system coupled to a Q-Exactive Orbitrap Plus mass spectrometer equipped with a nanoelectrospray ion source (Thermo Fisher Scientific, San Jose, CA, USA). The mass spectrometry (MS) raw files were searched against the Mouse Swiss-Prot Database

(17,138 proteins, November 2022) with a list of common protein contaminants. The search parameters were set for the following fixed modifications: carbamidomethylation of cysteine (+57.02146 Da), as well as light, medium, and heavy dimethylation of N termini and lysine (+28.031300, +32.056407, and +36.075670 Da) and variable modification: oxidation of methionine (15.99491 Da). The false positive discovery rate of the identified peptides based on Q-values using The Proteome Discoverer decoy database together with the Percolator algorithm was set to 1%. The relative MS signal intensities of dimethyl labeled peptides were quantified and presented as ratios of single LPS/no stimulation and LPS tolerance/no stimulation. Log 2 of the ratios in triplicate was used to calculate the *p*-values using Student's *t*-test. The proteins with a *p*-value < 0.05 were considered significant proteins, and these proteins were subjected to the online DAVID Bioinformatics Resources 6.8 to investigate the enriched biological processes. The mass spectrometry proteomics data have been deposited to the ProteomeXchange Consortium via the PRIDE partner repository with the dataset identifier PXD041265. Then, the data visualization was performed using R packages. Volcano plots were generated by ggplot2 version 3.4.2. KEGG pathway analyses were generated by PathfindR. Go enrichment analysis was performed using Shiny 0.77 (<http://bioinformatics.sdstate.edu/go/>) accessed on 20 March 2023.

4.6. Statistical Analysis

The results are shown as mean \pm S.E.M. All data were analyzed with GraphPad Prism6. Student's *t*-test or one-way analysis of variance [41] with Tukey's comparison test was used for the analysis of experiments with two and more than two groups, respectively. The survival analysis was determined by the log-rank test. For all datasets, a *p*-value less than 0.05 was considered significant.

5. Conclusions

The Ezh2-deleted macrophages induced fewer activities (proteomic and secretome analyses) after LPS stimulation compared with the control states, supporting the less severe sepsis in *Ezh2* null (*Ezh2^{fl/fl}; LysM-Cre^{cre/cre}*) over the control (*Ezh2^{fl/fl}; LysM-Cre^{-/-}*) mice. The more severe sepsis in CLP after LPS tolerance over CLP alone supported the less effective microbial control during LPS tolerance. The Ezh2 inhibitor was more effective in the CLP model than the CLP after LPS tolerance, perhaps due to the more profound sepsis severity in the latter condition. More studies on the use of Ezh2 blockage in sepsis are warranted.

Supplementary Materials: The following supporting information can be downloaded at: <https://www.mdpi.com/article/10.3390/ijms24108517/s1>.

Author Contributions: Conceptualization, N.H., T.P. and A.L.; methodology, P.P., J.M. and A.L.; formal analysis, P.P. and A.L.; investigation, P.P., P.K., J.M., J.I.-A., A.B., S.B., P.R. and A.N.-L.; resources, A.N.-L., N.H., T.P. and A.L.; data curation, P.P., J.M., J.I.-A. and A.L.; writing—original draft preparation, P.P. and A.L.; writing—review and editing, N.H., T.P. and A.L.; supervision, A.L.; funding acquisition, N.H. All authors have read and agreed to the published version of the manuscript.

Funding: This research was funded from NSRF via the Program Management Unit for Human Resources, Institutional Development, Research, and Innovation (B05F640144), (B16F640175), and (B36G660003) with Rachadapisek Sompote Matching Fund (RA-MF-04/66), and the Thailand Science research and Innovation Fund, Chulalongkorn University (CU_FRB65_heal (6)_012_32_07). This research was supported in part by the Intramural Research Program of National Institute of Allergy and Infectious Diseases (NIAID), National Institutes of Health (NIH). T.P. is funded by National Research Council of Thailand (811/2563). P.P. was supported by the Second Century Fund (C2F) for Postdoctoral Fellowship, Chulalongkorn University. P.K. was supported by the Second Century Fund (C2F) for high-efficiency Ph.D. candidates, Chulalongkorn University.

Institutional Review Board Statement: The study was conducted in accordance with the National Institutes of Health (NIH) criteria, and the animal study protocol was approved by the Institutional Animal Care and Use Committee of the Faculty of Medicine, Chulalongkorn University, Bangkok, Thailand (CU-ACUP No. 021/2562).

Informed Consent Statement: Not applicable.

Data Availability Statement: Not applicable.

Conflicts of Interest: The authors declare no conflict of interest.

References

1. Amornphimoltham, P.; Yuen, P.S.T.; Star, R.A.; Leelahavanichkul, A. Gut Leakage of Fungal-Derived Inflammatory Mediators: Part of a Gut-Liver-Kidney Axis in Bacterial Sepsis. *Dig. Dis. Sci.* **2019**, *64*, 2416–2428. [[CrossRef](#)]
2. Lacal, I.; Ventura, R. Epigenetic Inheritance: Concepts, Mechanisms and Perspectives. *Front. Mol. Neurosci.* **2018**, *11*, 292. [[CrossRef](#)] [[PubMed](#)]
3. Han, M.; Jia, L.; Lv, W.; Wang, L.; Cui, W. Epigenetic Enzyme Mutations: Role in Tumorigenesis and Molecular Inhibitors. *Front. Oncol.* **2019**, *9*, 194. [[CrossRef](#)] [[PubMed](#)]
4. Hotchkiss, R.S.; Moldawer, L.L.; Opal, S.M.; Reinhart, K.; Turnbull, I.R.; Vincent, J.L. Sepsis and septic shock. *Nat. Rev. Dis. Primers* **2016**, *2*, 16045. [[CrossRef](#)] [[PubMed](#)]
5. Liu, D.; Huang, S.-Y.; Sun, J.-H.; Zhang, H.-C.; Cai, Q.-L.; Gao, C.; Li, L.; Cao, J.; Xu, F.; Zhou, Y.; et al. Sepsis-induced immunosuppression: Mechanisms, diagnosis and current treatment options. *Mil. Med. Res.* **2022**, *9*, 56. [[CrossRef](#)] [[PubMed](#)]
6. Brady, J.; Horie, S.; Laffey, J.G. Role of the adaptive immune response in sepsis. *Intensive Care Med. Exp.* **2020**, *8*, 20. [[CrossRef](#)] [[PubMed](#)]
7. Delano, M.J.; Ward, P.A. Sepsis-induced immune dysfunction: Can immune therapies reduce mortality? *J. Clin. Investig.* **2016**, *126*, 23–31. [[CrossRef](#)] [[PubMed](#)]
8. Németh, K.; Leelahavanichkul, A.; Yuen, P.S.; Mayer, B.; Parmelee, A.; Doi, K.; Robey, P.G.; Leelahavanichkul, K.; Koller, B.H.; Brown, J.M.; et al. Bone marrow stromal cells attenuate sepsis via prostaglandin E(2)-dependent reprogramming of host macrophages to increase their interleukin-10 production. *Nat. Med.* **2009**, *15*, 42–49. [[CrossRef](#)]
9. Leelahavanichkul, A.; Yasuda, H.; Doi, K.; Hu, X.; Zhou, H.; Yuen, P.S.; Star, R.A. Methyl-2-acetamidoacrylate, an ethyl pyruvate analog, decreases sepsis-induced acute kidney injury in mice. *Am. J. Physiol. Renal Physiol.* **2008**, *295*, F1825–F1835. [[CrossRef](#)]
10. Taratummarat, S.; Sangphech, N.; Vu, C.T.B.; Palaga, T.; Ondee, T.; Surawut, S.; Sereemasapun, A.; Ritprajak, P.; Leelahavanichkul, A. Gold nanoparticles attenuates bacterial sepsis in cecal ligation and puncture mouse model through the induction of M2 macrophage polarization. *BMC Microbiol.* **2018**, *18*, 85. [[CrossRef](#)]
11. Panpetch, W.; Chanchaoenthana, W.; Bootdee, K.; Nilgate, S.; Finkelman, M.; Tumwasorn, S.; Leelahavanichkul, A. *Lactobacillus rhamnosus* L34 Attenuates Gut Translocation-Induced Bacterial Sepsis in Murine Models of Leaky Gut. *Infect. Immun.* **2018**, *86*, e00700-17. [[CrossRef](#)]
12. Issara-Amphorn, J.; Chanchaoenthana, W.; Visitchanakun, P.; Leelahavanichkul, A. Syk Inhibitor Attenuates Polymicrobial Sepsis in FcγRIIb-Deficient Lupus Mouse Model, the Impact of Lupus Characteristics in Sepsis. *J. Innate Immun.* **2020**, *12*, 461–479. [[CrossRef](#)] [[PubMed](#)]
13. Dang, C.P.; Leelahavanichkul, A. Over-expression of miR-223 induces M2 macrophage through glycolysis alteration and attenuates LPS-induced sepsis mouse model, the cell-based therapy in sepsis. *PLoS ONE* **2020**, *15*, e0236038. [[CrossRef](#)] [[PubMed](#)]
14. Chanchaoenthana, W.; Udompronpitak, K.; Manochantr, Y.; Kantagowit, P.; Kaewkanha, P.; Issara-Amphorn, J.; Leelahavanichkul, A. Repurposing of High-Dose Erythropoietin as a Potential Drug Attenuates Sepsis in Preconditioning Renal Injury. *Cells* **2021**, *10*, 3133. [[CrossRef](#)] [[PubMed](#)]
15. Dang, C.P.; Issara-Amphorn, J.; Charoensappakit, A.; Udompornpitak, K.; Bhunyakarnjanarat, T.; Saisorn, W.; Sae-Khow, K.; Leelahavanichkul, A. BAM15, a Mitochondrial Uncoupling Agent, Attenuates Inflammation in the LPS Injection Mouse Model: An Adjunctive Anti-Inflammation on Macrophages and Hepatocytes. *J. Innate Immun.* **2021**, *13*, 359–375. [[CrossRef](#)]
16. Perner, A.; Rhodes, A.; Venkatesh, B.; Angus, D.C.; Martin-Loeches, I.; Preiser, J.C.; Vincent, J.L.; Marshall, J.; Reinhart, K.; Joannidis, M.; et al. Sepsis: Frontiers in supportive care, organisation and research. *Intensive Care Med.* **2017**, *43*, 496–508. [[CrossRef](#)]
17. Mithal, L.B.; Arshad, M.; Swigart, L.R.; Khanolkar, A.; Ahmed, A.; Coates, B.M. Mechanisms and modulation of sepsis-induced immune dysfunction in children. *Pediatr. Res.* **2022**, *91*, 447–453. [[CrossRef](#)]
18. Schrijver, I.T.; Théroude, C.; Roger, T. Myeloid-Derived Suppressor Cells in Sepsis. *Front. Immunol.* **2019**, *10*, 327. [[CrossRef](#)]
19. Cao, C.; Ma, T.; Chai, Y.F.; Shou, S.T. The role of regulatory T cells in immune dysfunction during sepsis. *World J. Emerg. Med.* **2015**, *6*, 5–9. [[CrossRef](#)]
20. Vergadi, E.; Vaporidi, K.; Tsatsanis, C. Regulation of Endotoxin Tolerance and Compensatory Anti-inflammatory Response Syndrome by Non-coding RNAs. *Front. Immunol.* **2018**, *9*, 2705. [[CrossRef](#)]
21. Chanchaoenthana, W.; Sutnu, N.; Visitchanakun, P.; Sawaswong, V.; Chitcharoen, S.; Payungporn, S.; Schuetz, A.; Schultz, M.J.; Leelahavanichkul, A. Critical roles of sepsis-reshaped fecal virota in attenuating sepsis severity. *Front. Immunol.* **2022**, *13*, 940935. [[CrossRef](#)]
22. Chanchaoenthana, W.; Kamolratanakul, S.; Ariyanon, W.; Thanachartwet, V.; Phumratanaprapin, W.; Wilairatana, P.; Leelahavanichkul, A. Abnormal Blood Bacteriome, Gut Dysbiosis, and Progression to Severe Dengue Disease. *Front. Cell. Infect. Microbiol.* **2022**, *12*, 890817. [[CrossRef](#)]

23. Hiengrach, P.; Visitchanakun, P.; Tongchairawewat, P.; Tangsirisan, P.; Jungteerapanich, T.; Ritprajak, P.; Wannigama, D.L.; Tangtanatakul, P.; Leelahavanichkul, A. Sepsis Encephalopathy Is Partly Mediated by miR370-3p-Induced Mitochondrial Injury but Attenuated by BAM15 in Cecal Ligation and Puncture Sepsis Male Mice. *Int. J. Mol. Sci.* **2022**, *23*, 5445. [[CrossRef](#)]
24. Ondee, T.; Pongpirul, K.; Udompornpitak, K.; Sukkumee, W.; Lertmongkolaksorn, T.; Senaprom, S.; Leelahavanichkul, A. High Fructose Causes More Prominent Liver Steatohepatitis with Leaky Gut Similar to High Glucose Administration in Mice and Attenuation by *Lactiplantibacillus plantarum* dfa1. *Nutrients*. **2023**, *17*, 1462. [[CrossRef](#)]
25. Ondee, T.; Surawut, S.; Taratummarat, S.; Hirankarn, N.; Palaga, T.; Pisitkun, P.; Pisitkun, T.; Leelahavanichkul, A. Fc Gamma Receptor IIB Deficient Mice: A Lupus Model with Increased Endotoxin Tolerance-Related Sepsis Susceptibility. *Shock* **2017**, *47*, 743–752. [[CrossRef](#)] [[PubMed](#)]
26. Hiengrach, P.; Panpetch, W.; Chindamporn, A.; Leelahavanichkul, A. Macrophage depletion alters bacterial gut microbiota partly through fungal overgrowth in feces that worsens cecal ligation and puncture sepsis mice. *Sci. Rep.* **2022**, *12*, 9345. [[CrossRef](#)]
27. Makjaroen, J.; Thim-Uam, A.; Dang, C.P.; Pisitkun, T.; Sompan, P.; Leelahavanichkul, A. A Comparison Between 1 Day versus 7 Days of Sepsis in Mice with the Experiments on LPS-Activated Macrophages Support the Use of Intravenous Immunoglobulin for Sepsis Attenuation. *J. Inflamm. Res.* **2021**, *14*, 7243–7263. [[CrossRef](#)] [[PubMed](#)]
28. Kaewduangduen, W.; Visitchanakun, P.; Saisorn, W.; Phawadee, A.; Manonitnantawat, C.; Chutimaskul, C.; Susantitaphong, P.; Ritprajak, P.; Somboonna, N.; Cheibchalard, T.; et al. Blood Bacteria-Free DNA in Septic Mice Enhances LPS-Induced Inflammation in Mice through Macrophage Response. *Int. J. Mol. Sci.* **2022**, *23*, 1907. [[CrossRef](#)]
29. Visitchanakun, P.; Kaewduangduen, W.; Chareonsappakit, A.; Susantitaphong, P.; Pisitkun, P.; Ritprajak, P.; Townamchai, N.; Leelahavanichkul, A. Interference on Cytosolic DNA Activation Attenuates Sepsis Severity: Experiments on Cyclic GMP–AMP Synthase (cGAS) Deficient Mice. *Int. J. Mol. Sci.* **2021**, *22*, 11450. [[CrossRef](#)] [[PubMed](#)]
30. Doi, K.; Leelahavanichkul, A.; Yuen, P.S.; Star, R.A. Animal models of sepsis and sepsis-induced kidney injury. *J. Clin. Investig.* **2009**, *119*, 2868–2878. [[CrossRef](#)] [[PubMed](#)]
31. Vu, C.T.B.; Thammahong, A.; Yagita, H.; Azuma, M.; Hirankarn, N.; Ritprajak, P.; Leelahavanichkul, A. Blockade Of PD-1 Attenuated Postsepsis Aspergillosis Via The Activation of IFN-gamma and The Dampening of IL-10. *Shock* **2020**, *53*, 514–524. [[CrossRef](#)] [[PubMed](#)]
32. Walton, A.H.; Muenzer, J.T.; Rasche, D.; Boomer, J.S.; Sato, B.; Brownstein, B.H.; Pachot, A.; Brooks, T.L.; Deych, E.; Shannon, W.D.; et al. Reactivation of multiple viruses in patients with sepsis. *PLoS ONE* **2014**, *9*, e98819. [[CrossRef](#)] [[PubMed](#)]
33. Wang, T.; Derhovannessian, A.; De Cruz, S.; Belperio, J.A.; Deng, J.C.; Hoo, G.S. Subsequent infections in survivors of sepsis: Epidemiology and outcomes. *J. Intensive Care Med.* **2014**, *29*, 87–95. [[CrossRef](#)] [[PubMed](#)]
34. Seeley, J.J.; Ghosh, S. Molecular mechanisms of innate memory and tolerance to LPS. *J. Leukoc. Biol.* **2017**, *101*, 107–119. [[CrossRef](#)] [[PubMed](#)]
35. Gillen, J.; Ondee, T.; Gurusamy, D.; Issara-Amphorn, J.; Manes, N.P.; Yoon, S.H.; Leelahavanichkul, A.; Nita-Lazar, A. LPS Tolerance Inhibits Cellular Respiration and Induces Global Changes in the Macrophage Secretome. *Biomolecules* **2021**, *11*, 164. [[CrossRef](#)] [[PubMed](#)]
36. López-Collazo, E.; del Fresno, C. Pathophysiology of endotoxin tolerance: Mechanisms and clinical consequences. *Crit. Care* **2013**, *17*, 242. [[CrossRef](#)]
37. Naler, L.B.; Hsieh, Y.P.; Geng, S.; Zhou, Z.; Li, L.; Lu, C. Epigenomic and transcriptomic analyses reveal differences between low-grade inflammation and severe exhaustion in LPS-challenged murine monocytes. *Commun. Biol.* **2022**, *5*, 102. [[CrossRef](#)] [[PubMed](#)]
38. Koos, B.; Moderegger, E.L.; Rump, K.; Nowak, H.; Willemsen, K.; Holtkamp, C.; Thon, P.; Adamzik, M.; Rahmel, T. LPS-Induced Endotoxemia Evokes Epigenetic Alterations in Mitochondrial DNA That Impacts Inflammatory Response. *Cells* **2020**, *9*, 2282. [[CrossRef](#)]
39. Kunanopparat, A.; Leelahavanichkul, A.; Visitchanakun, P.; Kueanjinda, P.; Phuengmaung, P.; Sae-Khow, K.; Boonmee, A.; Benjaskulluecha, S.; Palaga, T.; Hirankarn, N. The Regulatory Roles of Ezh2 in Response to Lipopolysaccharide (LPS) in Macrophages and Mice with Conditional Ezh2 Deletion with LysM-Cre System. *Int. J. Mol. Sci.* **2023**, *24*, 5363. [[CrossRef](#)]
40. Falcao-Holanda, R.B.; Brunialti, M.K.C.; Jasiulionis, M.G.; Salomao, R. Epigenetic Regulation in Sepsis, Role in Pathophysiology and Therapeutic Perspective. *Front. Med.* **2021**, *8*, 685333. [[CrossRef](#)]
41. De Santa, F.; Narang, V.; Yap, Z.H.; Tusi, B.K.; Burgold, T.; Austenaa, L.; Bucci, G.; Caganova, M.; Notarbartolo, S.; Casola, S.; et al. Jmjd3 contributes to the control of gene expression in LPS-activated macrophages. *EMBO J.* **2009**, *28*, 3341–3352. [[CrossRef](#)]
42. De Santa, F.; Totaro, M.G.; Prosperini, E.; Notarbartolo, S.; Testa, G.; Natoli, G. The histone H3 lysine-27 demethylase Jmjd3 links inflammation to inhibition of polycomb-mediated gene silencing. *Cell* **2007**, *130*, 1083–1094. [[CrossRef](#)]
43. Kondo, T.; Ito, S.; Koseki, H. Polycomb in Transcriptional Phase Transition of Developmental Genes. *Trends Biochem. Sci.* **2016**, *41*, 9–19. [[CrossRef](#)] [[PubMed](#)]
44. Neele, A.E.; de Winther, M.P.J. Repressing the repressor: Ezh2 mediates macrophage activation. *J. Exp. Med.* **2018**, *215*, 1269–1271. [[CrossRef](#)]
45. Laugesen, A.; Hojfeldt, J.W.; Helin, K. Role of the Polycomb Repressive Complex 2 (PRC2) in Transcriptional Regulation and Cancer. *Cold Spring Harb. Perspect. Med.* **2016**, *6*, a026575. [[CrossRef](#)] [[PubMed](#)]
46. Tan, J.Z.; Yan, Y.; Wang, X.X.; Jiang, Y.; Xu, H.E. EZH2: Biology, disease, and structure-based drug discovery. *Acta Pharmacol. Sin.* **2014**, *35*, 161–174. [[CrossRef](#)] [[PubMed](#)]

47. Nakagawa, M.; Kitabayashi, I. Oncogenic roles of enhancer of zeste homolog 1/2 in hematological malignancies. *Cancer Sci.* **2018**, *109*, 2342–2348. [[CrossRef](#)]
48. Garber, K. Histone-writer cancer drugs enter center stage. *Nat. Biotechnol.* **2020**, *38*, 909–912. [[CrossRef](#)] [[PubMed](#)]
49. Liu, Y.; Peng, J.; Sun, T.; Li, N.; Zhang, L.; Ren, J.; Yuan, H.; Kan, S.; Pan, Q.; Li, X.; et al. Epithelial EZH2 serves as an epigenetic determinant in experimental colitis by inhibiting TNF α -mediated inflammation and apoptosis. *Proc. Natl. Acad. Sci. USA* **2017**, *114*, E3796–E3805. [[CrossRef](#)] [[PubMed](#)]
50. Neele, A.E.; Chen, H.J.; Gijbels, M.J.J.; van der Velden, S.; Hoeksema, M.A.; Boshuizen, M.C.S.; Van den Bossche, J.; Tool, A.T.; Matlung, H.L.; van den Berg, T.K.; et al. Myeloid Ezh2 Deficiency Limits Atherosclerosis Development. *Front. Immunol.* **2020**, *11*, 594603. [[CrossRef](#)]
51. Qin, H.; Holdbrooks, A.T.; Liu, Y.; Reynolds, S.L.; Yanagisawa, L.L.; Benveniste, E.N. SOCS3 deficiency promotes M1 macrophage polarization and inflammation. *J. Immunol.* **2012**, *189*, 3439–3448. [[CrossRef](#)]
52. Ruenjaiman, V.; Butta, P.; Leu, Y.W.; Pongpanich, M.; Leelahavanichkul, A.; Kueanjinda, P.; Palaga, T. Profile of Histone H3 Lysine 4 Trimethylation and the Effect of Lipopolysaccharide/Immune Complex-Activated Macrophages on Endotoxemia. *Front. Immunol.* **2019**, *10*, 2956. [[CrossRef](#)]
53. Benjaskulluecha, S.; Boonmee, A.; Pattarakankul, T.; Wongprom, B.; Klomsing, J.; Palaga, T. Screening of compounds to identify novel epigenetic regulatory factors that affect innate immune memory in macrophages. *Sci. Rep.* **2022**, *12*, 1912. [[CrossRef](#)] [[PubMed](#)]
54. Cheng, Y.; He, C.; Wang, M.; Ma, X.; Mo, F.; Yang, S.; Han, J.; Wei, X. Targeting epigenetic regulators for cancer therapy: Mechanisms and advances in clinical trials. *Signal. Transduct. Target. Ther.* **2019**, *4*, 62. [[CrossRef](#)]
55. Jaronwichawan, T.; Visitchanakun, P.; Dang, P.C.; Ritprajak, P.; Palaga, T.; Leelahavanichkul, A. Dysregulation of Lipid Metabolism in Macrophages Is Responsible for Severe Endotoxin Tolerance in Fc γ RIIB-Deficient Lupus Mice. *Front. Immunol.* **2020**, *11*, 959. [[CrossRef](#)] [[PubMed](#)]
56. Ondee, T.; Jaronwichawan, T.; Pisitkun, T.; Gillen, J.; Nita-Lazar, A.; Leelahavanichkul, A.; Somparn, P. Decreased Protein Kinase C- β Type II Associated with the Prominent Endotoxin Exhaustion in the Macrophage of Fc γ RIIB^{-/-} Lupus Prone Mice is Revealed by Phosphoproteomic Analysis. *Int. J. Mol. Sci.* **2019**, *20*, 1354. [[CrossRef](#)]
57. Thim-Uam, A.; Makjaroen, J.; Issara-Amphorn, J.; Saisorn, W.; Wannigama, D.L.; Chanchaoentana, W.; Leelahavanichkul, A. Enhanced Bacteremia in Dextran Sulfate-Induced Colitis in Splenectomy Mice Correlates with Gut Dysbiosis and LPS Tolerance. *Int. J. Mol. Sci.* **2022**, *23*, 1676. [[CrossRef](#)] [[PubMed](#)]
58. Duan, R.; Du, W.; Guo, W. EZH2: A novel target for cancer treatment. *J. Hematol. Oncol.* **2020**, *13*, 104. [[CrossRef](#)] [[PubMed](#)]
59. Carow, B.; Rottenberg, M.E. SOCS3, a Major Regulator of Infection and Inflammation. *Front. Immunol.* **2014**, *5*, 58. [[CrossRef](#)]
60. Zhang, X.; Wang, Y.; Yuan, J.; Li, N.; Pei, S.; Xu, J.; Luo, X.; Mao, C.; Liu, J.; Yu, T.; et al. Macrophage/microglial Ezh2 facilitates autoimmune inflammation through inhibition of Socs3. *J. Exp. Med.* **2018**, *215*, 1365–1382. [[CrossRef](#)]
61. Hu, G.; Guo, M.; Xu, J.; Wu, F.; Fan, J.; Huang, Q.; Yang, G.; Lv, Z.; Wang, X.; Jin, Y. Nanoparticles Targeting Macrophages as Potential Clinical Therapeutic Agents Against Cancer and Inflammation. *Front. Immunol.* **2019**, *10*, 1998. [[CrossRef](#)]
62. Tungsanga, S.; Panpetch, W.; Bhunyakarnjanarat, T.; Udompornpitak, K.; Katavetin, P.; Chanchaoentana, W.; Chatthanathon, P.; Somboonna, N.; Tungsanga, K.; Tumwasorn, S.; et al. Uremia-Induced Gut Barrier Defect in 5/6 Nephrectomized Mice Is Worsened by Candida Administration through a Synergy of Uremic Toxin, Lipopolysaccharide, and β -D-Glucan, but Is Attenuated by *Lactocaseibacillus rhamnosus* L34. *Int. J. Mol. Sci.* **2022**, *23*, 2511. [[CrossRef](#)] [[PubMed](#)]
63. Visitchanakun, P.; Panpetch, W.; Saisorn, W.; Chatthanathon, P.; Wannigama, D.L.; Thim-uam, A.; Svasti, S.; Fucharoen, S.; Somboonna, N.; Leelahavanichkul, A. Increased susceptibility to dextran sulfate-induced mucositis of iron-overload β -thalassemia mice, another endogenous cause of septicemia in thalassemia. *Clin. Sci.* **2021**, *135*, 1467–1486. [[CrossRef](#)]
64. Boonhai, S.; Bootdee, K.; Saisorn, W.; Takkavatakarn, K.; Sittichaoenchai, P.; Tungsanga, S.; Tiranathanagul, K.; Leelahavanichkul, A. TMAO reductase, a biomarker for gut permeability defect induced inflammation, in mouse model of chronic kidney disease and dextran sulfate solution-induced mucositis. *Asian Pac. J. Allergy Immunol.* **2021**. [[CrossRef](#)]
65. Binmama, S.; Dang, C.P.; Visitchanakun, P.; Hiengrach, P.; Somboonna, N.; Cheibchalard, T.; Pisitkun, P.; Chindamporn, A.; Leelahavanichkul, A. Beta-Glucan from *S. cerevisiae* Protected AOM-Induced Colon Cancer in cGAS-Deficient Mice Partly through Dectin-1-Manipulated Macrophage Cell Energy. *Int. J. Mol. Sci.* **2022**, *23*, 10951. [[CrossRef](#)]
66. Charoensappakit, A.; Sae-Khow, K.; Leelahavanichkul, A. Gut Barrier Damage and Gut Translocation of Pathogen Molecules in Lupus, an Impact of Innate Immunity (Macrophages and Neutrophils) in Autoimmune Disease. *Int. J. Mol. Sci.* **2022**, *23*, 8223. [[CrossRef](#)]
67. Ezponda, T.; Licht, J.D. Molecular pathways: Deregulation of histone h3 lysine 27 methylation in cancer-different paths, same destination. *Clin. Cancer Res.* **2014**, *20*, 5001–5008. [[CrossRef](#)]
68. Nichol, J.N.; Dupere-Richer, D.; Ezponda, T.; Licht, J.D.; Miller, W.H., Jr. H3K27 Methylation: A Focal Point of Epigenetic Deregulation in Cancer. *Adv. Cancer Res.* **2016**, *131*, 59–95. [[CrossRef](#)]
69. Yue, D.; Wang, Z.; Yang, Y.; Hu, Z.; Luo, G.; Wang, F. EZH2 inhibitor GSK343 inhibits sepsis-induced intestinal disorders. *Exp. Ther. Med.* **2021**, *21*, 437. [[CrossRef](#)] [[PubMed](#)]
70. Zhang, Q.; Sun, H.; Zhuang, S.; Liu, N.; Bao, X.; Liu, X.; Ren, H.; Lv, D.; Li, Z.; Bai, J.; et al. Novel pharmacological inhibition of EZH2 attenuates septic shock by altering innate inflammatory responses to sepsis. *Int. Immunopharmacol.* **2019**, *76*, 105899. [[CrossRef](#)] [[PubMed](#)]

71. Zhao, D.; Li, Z.; Liu, X.; Liu, N.; Bao, X.; Sun, H.; Meng, Q.; Ren, H.; Bai, J.; Zhou, X.; et al. Lymphocyte expression of EZH2 is associated with mortality and secondary infectious complications in sepsis. *Int. Immunopharmacol.* **2020**, *89*, 107042. [[CrossRef](#)]
72. Adema, V.; Colla, S. EZH2 Inhibitors: The Unpacking Revolution. *Cancer Res.* **2022**, *82*, 359–361. [[CrossRef](#)]
73. Wang, Q.; Xu, L.; Zhang, X.; Liu, D.; Wang, R. GSK343, an inhibitor of EZH2, mitigates fibrosis and inflammation mediated by HIF-1 α in human peritoneal mesothelial cells treated with high glucose. *Eur. J. Pharmacol.* **2020**, *880*, 173076. [[CrossRef](#)]
74. Bamidele, A.O.; Svingen, P.A.; Sagstetter, M.R.; Sarmiento, O.F.; Gonzalez, M.; Braga Neto, M.B.; Kugathasan, S.; Lomber, G.; Urrutia, R.A.; Faubion, W.A., Jr. Disruption of FOXP3-EZH2 Interaction Represents a Pathobiological Mechanism in Intestinal Inflammation. *Cell. Mol. Gastroenterol. Hepatol.* **2019**, *7*, 55–71. [[CrossRef](#)] [[PubMed](#)]
75. He, J.; Song, Y.; Li, G.; Xiao, P.; Liu, Y.; Xue, Y.; Cao, Q.; Tu, X.; Pan, T.; Jiang, Z.; et al. Fbxw7 increases CCL2/7 in CX3CR1hi macrophages to promote intestinal inflammation. *J. Clin. Investig.* **2019**, *129*, 3877–3893. [[CrossRef](#)]
76. Yong, H.; Wu, G.; Chen, J.; Liu, X.; Bai, Y.; Tang, N.; Liu, L.; Wei, J. lncRNA MALAT1 Accelerates Skeletal Muscle Cell Apoptosis and Inflammatory Response in Sepsis by Decreasing BRCA1 Expression by Recruiting EZH2. *Mol. Ther. Nucleic Acids* **2020**, *21*, 1120–1121. [[CrossRef](#)]
77. Alexander, W.S. Suppressors of cytokine signalling (SOCS) in the immune system. *Nat. Rev. Immunol.* **2002**, *2*, 410–416. [[CrossRef](#)] [[PubMed](#)]
78. Cassatella, M.A.; Gasperini, S.; Bovolenta, C.; Calzetti, F.; Vollebregt, M.; Scapini, P.; Marchi, M.; Suzuki, R.; Suzuki, A.; Yoshimura, A. Interleukin-10 (IL-10) selectively enhances CIS3/SOCS3 mRNA expression in human neutrophils: Evidence for an IL-10-induced pathway that is independent of STAT protein activation. *Blood* **1999**, *94*, 2880–2889. [[CrossRef](#)] [[PubMed](#)]
79. Prele, C.M.; Keith-Magee, A.L.; Yerkovich, S.T.; Murcha, M.; Hart, P.H. Suppressor of cytokine signalling-3 at pathological levels does not regulate lipopolysaccharide or interleukin-10 control of tumour necrosis factor- α production by human monocytes. *Immunology* **2006**, *119*, 8–17. [[CrossRef](#)]
80. Berlato, C.; Cassatella, M.A.; Kinjyo, I.; Gatto, L.; Yoshimura, A.; Bazzoni, F. Involvement of suppressor of cytokine signaling-3 as a mediator of the inhibitory effects of IL-10 on lipopolysaccharide-induced macrophage activation. *J. Immunol.* **2002**, *168*, 6404–6411. [[CrossRef](#)]
81. Qasimi, P.; Ming-Lum, A.; Ghanipour, A.; Ong, C.J.; Cox, M.E.; Ihle, J.; Cacalano, N.; Yoshimura, A.; Mui, A.L. Divergent mechanisms utilized by SOCS3 to mediate interleukin-10 inhibition of tumor necrosis factor α and nitric oxide production by macrophages. *J. Biol. Chem.* **2006**, *281*, 6316–6324. [[CrossRef](#)]
82. Mola, S.; Pinton, G.; Erreni, M.; Corazzari, M.; De Andrea, M.; Grolla, A.A.; Martini, V.; Moro, L.; Porta, C. Inhibition of the Histone Methyltransferase EZH2 Enhances Protumor Monocyte Recruitment in Human Mesothelioma Spheroids. *Int. J. Mol. Sci.* **2021**, *22*, 4391. [[CrossRef](#)] [[PubMed](#)]
83. Kitchen, G.B.; Hopwood, T.; Gali Ramamoorthy, T.; Downton, P.; Begley, N.; Hussell, T.; Dockrell, D.H.; Gibbs, J.E.; Ray, D.W.; Loudon, A.S.I. The histone methyltransferase Ezh2 restrains macrophage inflammatory responses. *FASEB J.* **2021**, *35*, e21843. [[CrossRef](#)]
84. Arango Duque, G.; Descoteaux, A. Macrophage cytokines: Involvement in immunity and infectious diseases. *Front. Immunol.* **2014**, *5*, 491. [[CrossRef](#)]
85. Wang, Y.; Wang, Q.; Wang, B.; Gu, Y.; Yu, H.; Yang, W.; Ren, X.; Qian, F.; Zhao, X.; Xiao, Y.; et al. Inhibition of EZH2 ameliorates bacteria-induced liver injury by repressing RUNX1 in dendritic cells. *Cell Death Dis.* **2020**, *11*, 1024. [[CrossRef](#)] [[PubMed](#)]
86. Kang, N.; Eccleston, M.; Clermont, P.L.; Latarani, M.; Male, D.K.; Wang, Y.; Crea, F. EZH2 inhibition: A promising strategy to prevent cancer immune editing. *Epigenomics* **2020**, *12*, 1457–1476. [[CrossRef](#)]
87. Makjaroen, J.; Phuengmaung, P.; Saisorn, W.; Udomkarnjananun, S.; Pisitkun, T.; Leelahavanichkul, A. Lipopolysaccharide Tolerance Enhances Murine Norovirus Reactivation: An Impact of Macrophages Mainly Evaluated by Proteomic Analysis. *Int. J. Mol. Sci.* **2023**, *24*, 1829. [[CrossRef](#)]
88. Leelahavanichkul, A.; Somporn, P.; Bootprapan, T.; Tu, H.; Tangtanatakul, P.; Nuengjumnong, R.; Worasilchai, N.; Tiranathanagul, K.; Eiam-ong, S.; Levine, M.; et al. High-dose ascorbate with low-dose amphotericin B attenuates severity of disease in a model of the reappearance of candidemia during sepsis in the mouse. *Am. J. Physiol. Regul. Integr. Comp. Physiol.* **2015**, *309*, R223–R234. [[CrossRef](#)]
89. Vu, C.T.B.; Thammahong, A.; Leelahavanichkul, A.; Ritprajak, P. Alteration of macrophage immune phenotype in a murine sepsis model is associated with susceptibility to secondary fungal infection. *Asian Pac. J. Allergy Immunol.* **2022**, *40*, 162–171. [[CrossRef](#)] [[PubMed](#)]
90. Ou, S.M.; Lee, K.H.; Tsai, M.T.; Tseng, W.C.; Chu, Y.C.; Tarng, D.C. Sepsis and the Risks of Long-Term Renal Adverse Outcomes in Patients With Chronic Kidney Disease. *Front. Med.* **2022**, *9*, 809292. [[CrossRef](#)]
91. Kalani, C.; Venigalla, T.; Bailey, J.; Udeani, G.; Surani, S. Sepsis Patients in Critical Care Units with Obesity: Is Obesity Protective? *Cureus* **2020**, *12*, e6929. [[CrossRef](#)] [[PubMed](#)]
92. Camilleri, M. Leaky gut: Mechanisms, measurement and clinical implications in humans. *Gut* **2019**, *68*, 1516–1526. [[CrossRef](#)]
93. de Kort, S.; Keszthelyi, D.; Masclee, A.A. Leaky gut and diabetes mellitus: What is the link? *Obes. Rev.* **2011**, *12*, 449–458. [[CrossRef](#)]
94. Costantini, E.; Carlin, M.; Porta, M.; Brizzi, M.F. Type 2 diabetes mellitus and sepsis: State of the art, certainties and missing evidence. *Acta Diabetol.* **2021**, *58*, 1139–1151. [[CrossRef](#)] [[PubMed](#)]

95. Colbert, J.F.; Schmidt, E.P.; Faubel, S.; Ginde, A.A. Severe Sepsis Outcomes Among Hospitalizations With Inflammatory Bowel Disease. *Shock* **2017**, *47*, 128–131. [[CrossRef](#)]
96. Arbuckle, J.H.; Gardina, P.J.; Gordon, D.N.; Hickman, H.D.; Yewdell, J.W.; Pierson, T.C.; Myers, T.G.; Kristie, T.M. Inhibitors of the Histone Methyltransferases EZH2/1 Induce a Potent Antiviral State and Suppress Infection by Diverse Viral Pathogens. *mBio* **2017**, *8*, e01141-17. [[CrossRef](#)]
97. Martinez, M.L.; Plata-Menchaca, E.P.; Ruiz-Rodriguez, J.C.; Ferrer, R. An approach to antibiotic treatment in patients with sepsis. *J. Thorac. Dis.* **2020**, *12*, 1007–1021. [[CrossRef](#)]
98. Visitchanakun, P.; Tangtanatakul, P.; Trithiphen, O.; Soonthornchai, W.; Wongphoom, J.; Tachaboon, S.; Srisawat, N.; Leelahavanichkul, A. Plasma miR-370-3P as a Biomarker of Sepsis-Associated Encephalopathy, the Transcriptomic Profiling Analysis of MicroRNA-Arrays From Mouse Brains. *Shock* **2020**, *54*, 347–357. [[CrossRef](#)]
99. Issara-Amphorn, J.; Surawut, S.; Worasilchai, N.; Thim-Uam, A.; Finkelman, M.; Chindamporn, A.; Palaga, T.; Hirankarn, N.; Pisitkun, P.; Leelahavanichkul, A. The Synergy of Endotoxin and (1→3)-β-D-Glucan, from Gut Translocation, Worsens Sepsis Severity in a Lupus Model of Fc Gamma Receptor IIb-Deficient Mice. *J. Innate Immun.* **2018**, *10*, 189–201. [[CrossRef](#)]
100. Panpetch, W.; Somboonna, N.; Bulan, D.E.; Issara-Amphorn, J.; Finkelman, M.; Worasilchai, N.; Chindamporn, A.; Palaga, T.; Tumwasorn, S.; Leelahavanichkul, A. Oral administration of live- or heat-killed *Candida albicans* worsened cecal ligation and puncture sepsis in a murine model possibly due to an increased serum (1→3)-β-D-glucan. *PLoS ONE* **2017**, *12*, e0181439. [[CrossRef](#)] [[PubMed](#)]
101. Hiengrach, P.; Visitchanakun, P.; Finkelman, M.A.; Chanchaoenthana, W.; Leelahavanichkul, A. More Prominent Inflammatory Response to Pachyman than to Whole-Glucan Particle and Oat-β-Glucans in Dextran Sulfate-Induced Mucositis Mice and Mouse Injection through Proinflammatory Macrophages. *Int. J. Mol. Sci.* **2022**, *23*, 4026. [[CrossRef](#)]
102. Singkham-In, U.; Phuengmaung, P.; Makjaroen, J.; Saisorn, W.; Bhunyakarnjanarat, T.; Chatsuwan, T.; Chirathaworn, C.; Chanchaoenthana, W.; Leelahavanichkul, A. Chlorhexidine Promotes Psl Expression in *Pseudomonas aeruginosa* That Enhances Cell Aggregation with Preserved Pathogenicity Demonstrates an Adaptation against Antiseptic. *Int. J. Mol. Sci.* **2022**, *23*, 8308. [[CrossRef](#)]
103. Udornpornpitak, K.; Charoensappakit, A.; Sae-Khow, K.; Bhunyakarnjanarat, T.; Dang, C.P.; Saisorn, W.; Visitchanakun, P.; Phuengmaung, P.; Palaga, T.; Ritprajak, P.; et al. Obesity Exacerbates Lupus Activity in Fc Gamma Receptor IIb Deficient Lupus Mice Partly through Saturated Fatty Acid-Induced Gut Barrier Defect and Systemic Inflammation. *J. Innate Immun.* **2022**, *15*, 240–261. [[CrossRef](#)]
104. Ondee, T.; Gillen, J.; Visitchanakun, P.; Somparn, P.; Issara-Amphorn, J.; Dang Phi, C.; Chanchaoenthana, W.; Gurusamy, D.; Nita-Lazar, A.; Leelahavanichkul, A. Lipocalin-2 (Lcn-2) Attenuates Polymicrobial Sepsis with LPS Preconditioning (LPS Tolerance) in FcγRIIb Deficient Lupus Mice. *Cells* **2019**, *8*, 1064. [[CrossRef](#)] [[PubMed](#)]
105. Hiengrach, P.; Panpetch, W.; Chindamporn, A.; Leelahavanichkul, A. *Helicobacter pylori*, Protected from Antibiotics and Stresses Inside *Candida albicans* Vacuoles, Cause Gastritis in Mice. *Int. J. Mol. Sci.* **2022**, *23*, 8568. [[CrossRef](#)] [[PubMed](#)]
106. Panpetch, W.; Visitchanakun, P.; Saisorn, W.; Sawatpanich, A.; Chatthanathon, P.; Somboonna, N.; Tumwasorn, S.; Leelahavanichkul, A. *Lactobacillus rhamnosus* attenuates Thai chili extracts induced gut inflammation and dysbiosis despite capsaicin bactericidal effect against the probiotics, a possible toxicity of high dose capsaicin. *PLoS ONE* **2021**, *16*, e0261189. [[CrossRef](#)]
107. Phuengmaung, P.; Mekjaroen, J.; Saisorn, W.; Chatsuwan, T.; Somparn, P.; Leelahavanichkul, A. Rapid Synergistic Biofilm Production of *Pseudomonas* and *Candida* on the Pulmonary Cell Surface and in Mice, a Possible Cause of Chronic Mixed Organismal Lung Lesions. *Int. J. Mol. Sci.* **2022**, *23*, 9202. [[CrossRef](#)] [[PubMed](#)]

Disclaimer/Publisher’s Note: The statements, opinions and data contained in all publications are solely those of the individual author(s) and contributor(s) and not of MDPI and/or the editor(s). MDPI and/or the editor(s) disclaim responsibility for any injury to people or property resulting from any ideas, methods, instructions or products referred to in the content.